83
SUR/FIN

American Electroplaters' Society SUR/FIN '83

70th Annual Technical Conference

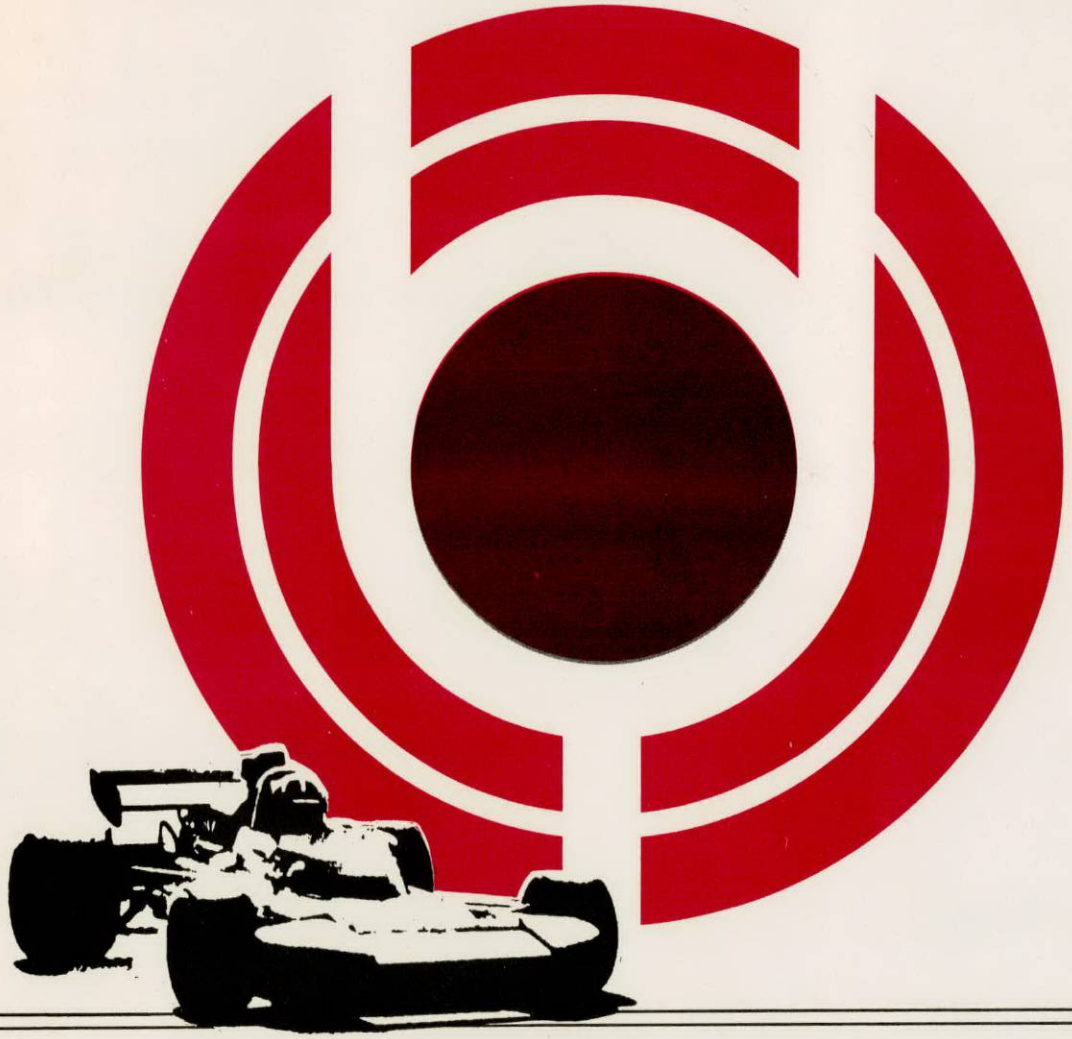

June 27-30, 1983
Hyatt Regency Indianapolis and
The Indiana Convention - Exposition Center
Indianapolis, IN

SESSION H

AMERICAN ELECTROPLATERS' SOCIETY, INC.

70TH ANNUAL TECHNICAL CONFERENCE - INDIANAPOLIS, IN

ELECTROLESS PLATING

SESSION H

Page No.

The Relationship Between Stress and Adhesion of Electroless Nickel-Phosphorus Deposits on Zincated Aluminum.....H-1

Glenn O. Mallory, Allied-Kelite Div., Witco Chemical Corp., Los Angeles, CA

Performance of Electroless Deposits for EMI/RFI Shielding Applications.....H-2

Gerald Krulik and John Waggoner, Enthone, Inc., Bridgeview, IL

Using Computer Technology in Electroless Nickel.....H-3

Phillip D. Stapleton, Stapleton Company, Long Beach, CA

Electroless Gold.....H-4

Dr. Raichur Narayan, TRW Connectors, Elk Grove Village, IL

Electroless Nickel for Stress Corrosion Protection in Power and Petrochemical Plants.....H-5

Gabrielle Salvago and D. Sinigaglia, Dipartimento di Chimica Fisica, Politecnico di Milano, Milano, Italy

Diverse Applications for Electroless Tin.....H-6

Jack Fellman, CuTech, Inc., Hatfield, PA

H-1

Electroless Plating Session H

The Relationship Between Stress and Adhesion of Electroless Nickel-Phosphorus Deposits on Zincated Aluminum

Glenn O. Mallory
Allied-Kelite Div.
Witco Chemical Corp.
Los Angeles, CA

The Relationship Between Stress And Adhesion Of Electroless Nickel-Phosphorus Deposits On Zincated Aluminum

Glenn O. Mallory
Allied-Kelite Div., Witco Chemical Corp.
Los Angeles, CA 90012

ABSTRACT

Several factors affecting the adhesion of electroless nickel-phosphorus deposits on zincated aluminum were studied. The two most important factors affecting adhesion were found to be the formation of a zinc rich zone (ZRZ) at the Ni-Al interface and deposit stress. Additionally, deposits that have high internal tensile stress are shown to induce adhesion failure when the ZRZ is relatively thick. The induction time for electroless nickel deposition is shown to be related to the thickness of the zinc film. The structure and composition of the Ni-Al interface were determined by AES analysis.

Two models for adhesion failure of the electroless nickel plated aluminum are proposed.

INTRODUCTION

Metallic coatings, such as nickel, applied to aluminum alloys by electrolytic or electroless deposition provide properties that include corrosion protection, abrasion and wear resistance, solderability, and enhanced aesthetic appeal. Additionally, the chemical and physical properties of electroless nickel-phosphorus deposits provide several more advantages over electrodeposited nickel. Electroless nickel (EN) will deposit uniformly over complex shapes. Electroless Ni-P deposits in the as-plated condition have hardness values in the range of 500 to 600 VHN compared to 200 to 300 VHN for typical nickel electrodeposits. Electroless Ni-P alloys generally exhibit superior resistance to chemical attack when compared to "pure" nickel deposits. However, aluminum and its alloys are anodic to the metals that are commonly plated onto it. Galvanic corrosion of the aluminum can occur when the substrate is exposed to a hostile environment through pores in the plated deposit. Electroless nickel plating provides a coating with inherent low porosity.

Concomitant with the enhanced properties obtained when aluminum is plated with nickel is the difficulty encountered in plating the substrate. Aluminum has a natural affinity for oxygen, hence there is an oxide film always present on the aluminum surface. The kinetics for formation of the oxide is such that if the film is removed it reforms immediately regardless of the surface preparation process. This "permanent" oxide film interferes with the formation of metallic bonds between the aluminum substrate and the metal deposit. The aluminum must be protected from re-oxidation between the removal of the oxide and the deposition process. The oxide film can be replaced by simple immersion deposition of another metal on aluminum. This thin metallic film, usually zinc, must be resistant to oxidation. The conventional method of applying the zinc film involves immersing the aluminum substrate in an alkaline zincate solution.

The alkaline zinc immersion process was first described by Hewitson in 1927[1]. Several years later, modifications of the process were reported by Korpium[2] in 1939 and Perner[3] in 1942.

The overall alkaline zinc immersion process can be characterized as follows:

1. Dissolution of aluminum (anodic)

(1) $Al + 3OH^- = Al(OH)_3 + 3e^-$, $E^0 = 2.31$

$Al(OH)_3 = H_2AlO_3^- + H^+$

2. Deposition of zinc (cathodic)

(2) $Zn(OH)_4 = Zn^{++} + 4OH^-$

$Zn^{++} + 2e^- = Zn^0$, $E^0 = -0.763$

$H^+ + e^- = 1/2H_2$

There are two general types of alkaline zincate solutions:

1. Concentrated

Zinc oxide — 40-100 grams per litre

Sodium hydroxide — 400-550 grams per litre

2. Dilute

Zinc oxide — 5-20 grams per litre

Sodium hydroxide — 50-120 grams per litre

These two general formulations have been further modified by the addition of various metal ions such as iron, nickel, lead or copper, along with various chelating agents; e.g., gluconates, tartrates, etc.[4] Several proprietary products are available that are based on these modifications.

A study of the corrosion of zincated, plated aluminum by W. G. Zelley[5] led him to the conclusion that the best results are obtained with the thinnest immersion zinc deposits practicable.

Keller and Zelley[6] showed the effect of temperature and alloy on the weight of the immersion zinc film formed on the aluminum alloy. Figure 1 shows the variation in weight of zinc deposited with temperature. The higher the temperature, the more zinc deposited.

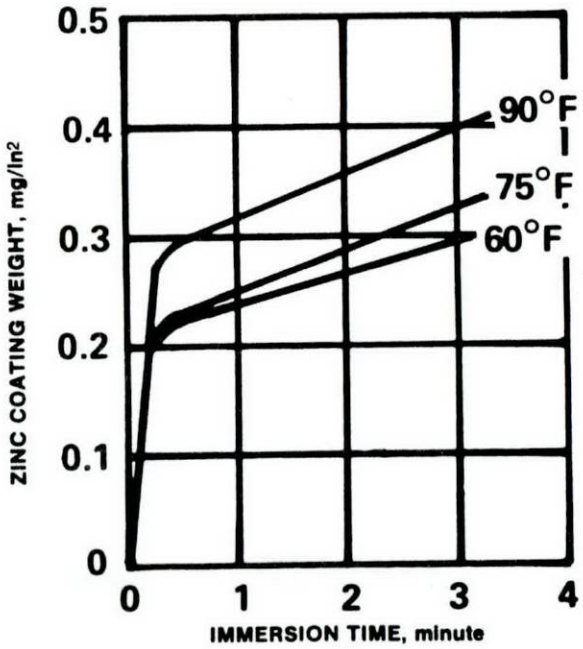

Figure 1. Effect of temperature of zincate solution on weight of zinc film deposited on 1100-H18 aluminum sheet.

Figure 2 shows the effect of the alloy on the zinc immersion coating weight. This effect is due to the differences in potential between the aluminum alloys and zinc in the zincate solution. The greater the potential difference, the heavier the zinc deposit.

For those alloys that yield a zinc film that is heavier than desired, the double zinc immersion process described by Korpium[2] can be used to produce thinner deposits. A typical process sequence involves:

1. Solvent clean
2. Mild alkaline clean
3. Rinse
4. Deoxidize
5. Rinse
6. Zincate for 60 seconds at room temperature
7. Rinse
8. Remove zinc film in 50% nitric acid
9. Rinse
10. Final zincate for 30 to 60 seconds at room temperature

In 1949, Heiman[7] reported an acid zinc immersion system for plating on aluminum. He proposed a solution containing zinc sulfate and hydrofluoric acid, for example:

$ZnSO_4 \cdot 7H_2O$ — 720 grams per litre
HF (48%) — 17.5 mL per litre

Heiman recommended operating this solution at room temperature with immersion times up to one minute. The acid zinc immersion process can also be characterized by an anodic step and a cathodic step as follows:

1. Anodic

(3) $Al + 6F^- = AlF_6^{---} + 3e^-, \quad E^0 = 2.07$

2. Cathodic

(4) $Zn^{++} + 2e^- = Zn, \quad E^0 = -0.763$

$H^+ + e^- = 1/2H_2$

Figure 3 shows the variation of weight of zinc deposited from an acid zinc immersion bath on aluminum alloys 2024, 6061 and 7075. The order of increasing deposit weight as

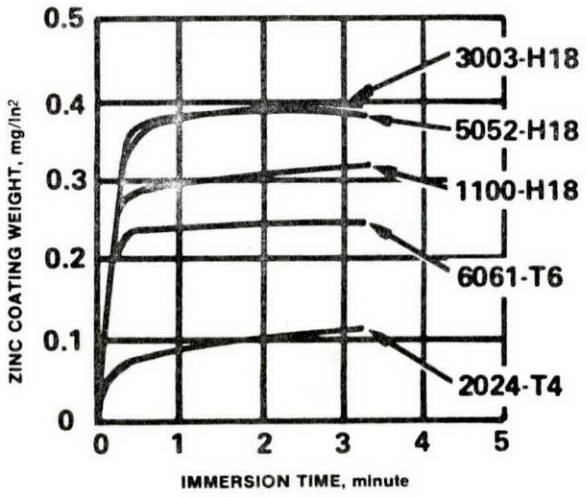

Figure 2. Weight of zinc film obtained from the alkaline zinc immersion process.

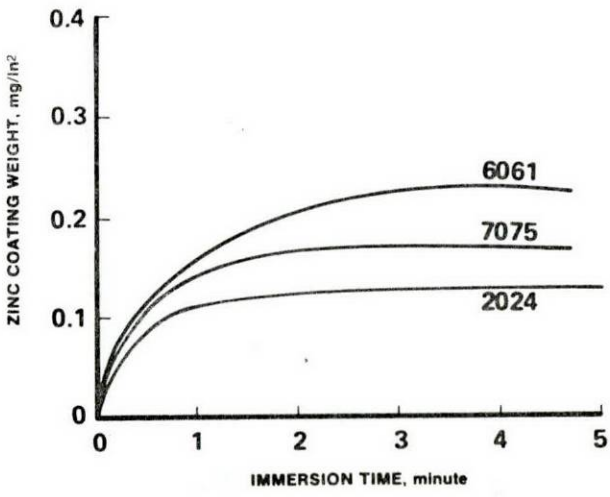

Figure 3. Weight of zinc film obtained from acid zinc immersion bath.

with the alkaline zincate systems is: 2024 < 7075 < 6061. By comparing the weight results obtained for alkaline zincate solutions and the acid Heiman solution, it is seen that much shorter immersion times are required for alkaline zincates than for acid zinc solutions.

In spite of the development and availability of well-researched commercial immersion zinc processes, electroless nickel deposits are known to develop poor adhesion to zincated aluminum surfaces. Blackwood et al[8] state that adhesion is directly related to the zincating solution, the composition of the aluminum alloy, and the electroless nickel bath itself. Yarkosky and coworkers[9] claim that adhesion failure results from the increase in total acidity of the plating bath. Other investigators indicate that the adhesion of the coating to the substrate is influenced by the nature and magnitude of the internal stress of the EN deposit. In general, a tensile stress in the coating will decrease its adhesion, corrosion resistance and sometimes the fatigue strength of the substrate. The objective of this paper is the study of the nature of the internal stress of EN deposits and its effect on the adhesion of the deposits to zincated aluminum.

EXPERIMENTAL

Aluminum Substrates

Five aluminum alloys were used in this study: 1100, 2024, 3003, 5086 and 6061. Alloy 1100 was used in all Auger Electron Spectroscopy (AES) analyses because of its purity. That is, the dissolution of an aluminum substrate in the zincate solution will leave traces of the alloying constituent at the interface of the zinc film and the aluminum. AES analysis cannot discriminate between copper from dissolution of alloy 2024 or residual copper from the copper bearing zincate solution. The aluminum helices used on the spiral contractometer stress tests were alloy 3003. Adhesion, AES and salt spray tests were run on either 4 in × 2 in × .030 in or 6 in × 4 in × .020 in panels. The composition of each alloy is given in Table 1.

Table 1. Nominal Composition Of Aluminum Alloys; Essential Elements (Percent By Weight)

Alloy	Cu	Mn	Si	Mg	Zn	Fe	Cr
1100	—	—	—	—	—	—	—
2024	4.5	0.6	0.5	1.5	0.2	0.5	0.1
3003	0.1	1.2	0.6	—	0.1	0.7	—
5086	0.1	0.5	0.4	4	0.25	0.5	0.1
6061	0.25	0.1	0.6	1.0	0.25	0.7	0.25

Process Cycle

1. Clean in proprietary acid cleaner
2. Cold water rinse
3. Acid etch
   - HNO_3 — 50% by vol.
   - H_2SO_4 — 25% by vol.
   - NH_4HF_2 — 120 g/L
   - Water — Balance
4. Cold water rinse
5. Zincate, 30 seconds
6. Electroless nickel plate

Zincate Solutions

Three zincate solutions were used to prepare the aluminum for plating. The formulations of the alkaline zincate solutions are recorded in Table 2. The immersion time in the zincate solutions was 30 seconds.

Table 2. Formulations Of Test Zincate Solutions A, B and C

Material	Concentration, g/L A	B*	C*
NaOH	100	500	100
ZnO	15	100	15
CuCN	—	20	—
KCN	—	45	—
$FeCl_3 \cdot 6H_2O$	1.5	—	—
Sodium Gluconate	5	—	5
Catechol	5	—	5

* See Reference 4

EN Plating Bath

A 4-litre plating bath was used for all plating tests. The surface area-to-solution volume ratio was kept at 30 cm^2/litre (except for stress tests) to minimize the effects of changes in bath composition during the course of the plating test. The composition of the reference plating solution used in this investigation is given below:

Bath Composition		
Ni	—	0.1 M
Lactic Acid	—	0.3 M
Acetic Acid	—	0.25 M
Sodium Acetate	—	0.25 M
$NaH_2PO_2 \cdot H_2O$	—	0.3M
pH	—	Variable (4.0-5.2), adjust with dilute NaOH
Temperature	—	88° C
Thiourea	—	As required
Lead	—	As required

The stabilizers were added to the reference solution as required. The acetic acid/acetate buffer system was used to minimize pH changes during each experimental run. The pH did not vary more than 0.03 pH units from any given initial value. All panels were plated to a thickness of 25 μm (1.0 mil).

Stress Tests

The type and magnitude of internal stresses in EN deposits were determined with a Brenner-Senderoff Contractometer. In essence, the method of measuring the stress is based on plating the outside of a helix, which in operation has one end fixed and the other

end is allowed to move as the stress develops. The free end transmits its movement to an indicating needle through gears that magnify the needle movement. As the helix is EN plated, the stress in the deposit causes the helix to wind more tightly if the stress is compressive or unwind if the stress is tensile. The internal stress can be calculated from the amount of needle deflection and other data. For the stress calculation, the calibration constant of the helix must be known, and consists essentially of determining the force required per degree of dial deflection.

The range of the instrument is approximately 20,000 psi tensile (or compressive) when the stud in the gear is in line with the axis of the gears. This range can be doubled for a solution in which stress is known to be highly tensile (or compressive) by positioning the gear to the left for tensile solutions or to the right for compressive solutions.

The calculation of stress, σ, from the angular deflection, δ, is based on the equation,

$$\sigma = \frac{ET\,(T+t)\rho\delta}{6\pi\ DLt} \tag{5}$$

where,

E = modulus of elasticity of substrate
T = thickness of helix
t = thickness of deposit
ρ = pitch of the helix
δ = angular deflection
D = outer diameter of helix
L = length of helix

Stress measurements taken at operating temperature of the plating bath are related to the intrinsic stress. Stress measurements made after the contractometer system has cooled to room temperature are reported as the total or residual stress.

Potential-Time Measurements

Potential-time (E-t) tests were performed using a PAR Model 350 corrosion measurement system adapted for chronopotentiometric measurements.

Adhesion Tests

Adhesion failure was determined visually. That is, the surface of plated panels were examined for any evidence of blisters, cracks or exfoliated deposits. Blister formation during plating and salt spray testing was also monitored. The type of failure (cohesive or adhesive) was determined by AES analysis.

The simplest and most common test of adhesion is the bend test. However, there are many variables other than stress that affect adhesion in this method of testing. Hence, the bend test was used sparingly and only when it was felt that a qualitative check was necessary.

AES Analysis

All AES analytical tests were performed by Surface Science Laboratories, Inc., Mountain View, California.

DISCUSSION

Zinc Film Formation

Data derived from studies on the weight of zinc film deposited versus time for the three experimental zincate solutions closely parallels the results obtained by other investigators.

The concentrated zincate solution (B) produces the heaviest zinc films on all alloys. The inhibited dilute zincate solution (A) yields the thinnest deposits. The uninhibited dilute zincate solution (C) produces deposits that are, weightwise, between those of A and B. In general, the weight of films obtained from solution C are closer to deposits from solution A than solution B.

Wyszynski[10] showed that the rate of zinc film growth from uninhibited zincate solutions was much greater than that yielded by inhibited (Fe-complex) solutions. Lashmore[11] demonstrated that small additions of metal ions, e.g., Fe^{+3}, to zincate solutions have a major effect on the zinc immersion reaction. He found that in the presence of a ferric complex, the dissolution of aluminum occurs at a rate of nine atoms of aluminum for each zinc atom deposited. In the absence of the iron-complex, three atoms of aluminum dissolve for every two atoms of zinc deposited. Typical weight versus time curves for the experimental zincates are shown in Figure 4. The aluminum alloy is 1100.

Zinc Film Dissolution

Dissolution of the zinc film occurs when the zincated aluminum substrate is immersed in the EN plating bath. However, zinc metal is not simply dissolved chemically and then dispersed throughout the bulk of the EN solution. Zinc and other metal ions are reduced and codeposited with nickel into the EN deposit. This is demonstrated by AES analysis over the Ni-P/aluminum substrate interface. A zinc rich zone (ZRZ) is shown to exist between the bulk EN deposit and the aluminum surface. The elemental components and thicknesses of the ZRZ's are given in Table 3.

Table 3. Elemental Composition And Thickness Of Residual ZRZ

Zincate Solution	ZRZ Thickness, Å	ZRZ Elemental Composition Zn	Ni	P	Al	Fe	Cu
A	665	+	+	+	+	+	0
B	2500	+	+	+	+	0	+
C	1500	+	+	+	+	0	0

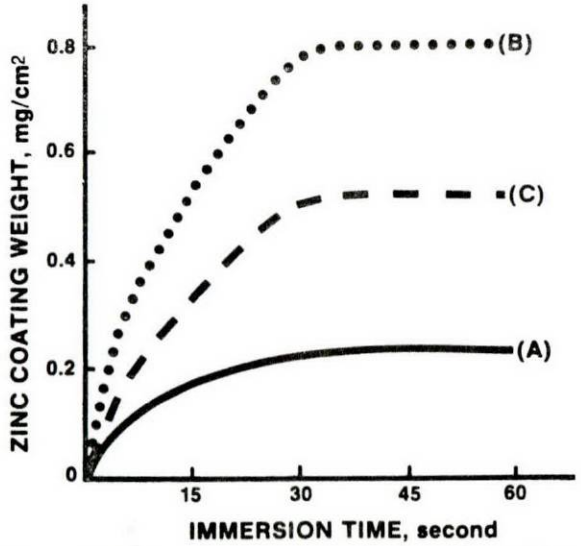

Figure 4. Weight of zinc film obtained from the three zincate solutions on alloy 1100.

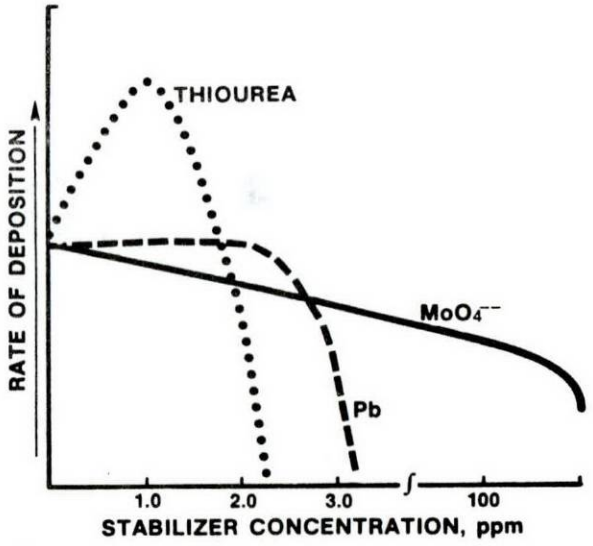

Figure. 5. Effect of stabilizer concentration on rate of electroless deposition.

Zinc Rich Zones (ZRZ)

The thickness and composition of a ZRZ depends mainly on three factors:

1. Composition of the zincate solution
2. Composition of the aluminum alloy
3. Chemistry of the EN plating bath

The results given in Table 3 reflect the effect of the composition of the zincate solution on the formation of the residual ZRZ. The EN plating bath contained no stabilizers and the aluminum substrate was 1100 alloy (certified to be 99.9% pure).

Comparison of ZRZ thicknesses show that the concentrated zincate (solution B) results in the thickest ZRZ, followed by solution C. Dissolution of the zinc film formed from solution A yields the thinnest ZRZ. It should be noted that solutions A and C differ only in that A contains the iron-complex.

In Figure 2 it was seen that the weight of zinc deposited in a given time period was influenced by the aluminum alloy being processed. It can be safely stated that alloys which catalyze the formation of heavy zinc films will also retain the thickest ZRZ.

The addition of certain stabilizers to the EN plating bath has a pronounced effect on mass transport during the dissolution-codeposition reactions involving the zinc film at the interface. AES depth profiles of solution A's ZRZ showed the zinc to be much thinner when 1 ppm thiourea was added to the EN plating bath. No change in zinc thickness was observed when the stabilizer was 1 ppm lead. The addition of oxy-anion stabilizers, e.g., IO_3^- or MoO_4^{--}, lead to an expanded ZRZ. These results are tabulated in Table 4.

Table 4. Effect Of Stabilizers On ZRZ Thickness

Zincate Solutions	ZRZ Thickness, Å			
	Neat	Thiourea	Pb	MoO_4
A	665	250	670	900
B	2500	1400	2300	2900
C	1500	800	1400	1800

The effect of the stabilizers on the rate of nickel deposition is shown in Figure 5. At its optimum concentration, thiourea has a marked accelerating effect on the deposition rate. It is assumed that when thiourea is added, the rate of EN deposition exceeds the rate of zinc dissolution relative to the rate without thiourea. In this case, the perpendicular distance the zinc ions migrate from the aluminum substrate is minimal, resulting in a thin ZRZ. Lead as a stabilizer has little or no effect on the deposition rate up to its critical concentration, hence no change in ZRZ from the zero stabilizer case. The oxy-anion stabilizers tend to reduce EN deposition rate in the concentration range where they are effective stabilizers, allowing the zinc ions to diffuse a greater distance from the aluminum surface, thereby expanding the ZRZ.

Induction Time for EN Deposition

The time required for establishment of the steady-state mixed (deposition) potential, E_d, is call the induction time. When EN plating zincated aluminum, the induction time was observed to be dependent on several variables. These factors include the weight of the zinc film, the aluminum alloy substrate, and the chemistry of the plating bath. The first two variables are interdependent. The weight of the zinc film on a particular aluminum alloy depends on the type of zincate solution used. On the other hand, the aluminum alloy

influences the weight of the zinc film formed from a given zincate solution (see Figure 2). The discussion that follows is limited to the experimental data obtained for one aluminum alloy, 1100. The results are typical of all the aluminum alloys studied.

Potential-time (E-t) curves for the zincated 1100 alloy are shown in Figure 6. The (E-t) curves exhibit a sudden change of potential when E_d is reached. The time necessary to reach the deposition potential is termed the induction time. The induction time depends on the weight of the zinc film formed.

The initial potentials of zincated aluminum in the EN plating bath are always more negative than E_d.

The zinc dissolution reaction takes place during the induction period. This reaction is accompanied by the immersion deposition of nickel. That is,

$$\begin{aligned} \text{Zn dissolution reaction:} \quad & Zn^0 = Zn^{++} + 2e^- , \; E^0 = 0.763 \\ \text{Ni immersion deposition:} \quad & Ni^{++} + 2e^- = Ni^0 , \; E^0 = -0.250 \\ \hline \text{Overall reaction:} \quad & Zn^0 + Ni^{++} = Ni^0 + Zn^{++} , \; E^0 = 0.513 \end{aligned}$$

The initial potential measured when zincated aluminum is immersed in the EN plating bath is equivalent to the potential reading obtained when zinc foil (99.99) is immersed in the EN solution. The potential, in the latter case, changes in the direction of E_d for the EN reaction. Since zinc is not catalytic to EN deposition, E_d is never attained. However, the potential drift to more positive values does indicate that the displacement reaction between zinc metal and nickel ions is proceeding. (E-t) curve for zinc foil in the EN plating solution is shown in Figure 7.

The previous discussion on zinc film dissolution indicated that the zinc metal is not simply dissolved but is subsequently codeposited with nickel into the EN film, forming a zinc rich zone, the ZRZ. The question arises as to how the thermodynamic driving force for zinc dissolution can coexist with the driving force for zinc deposition, both in the same electrode potential. The answer may lie in the Nernst relationship for the zinc reaction:

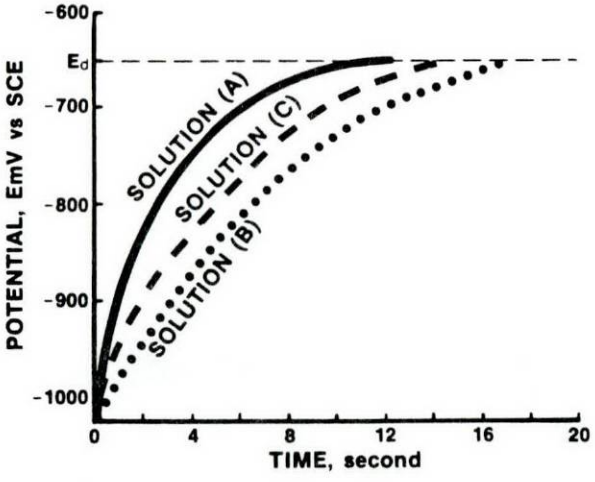

Figure 6. Potential-time curves for electroless nickel deposition on zincated aluminum.

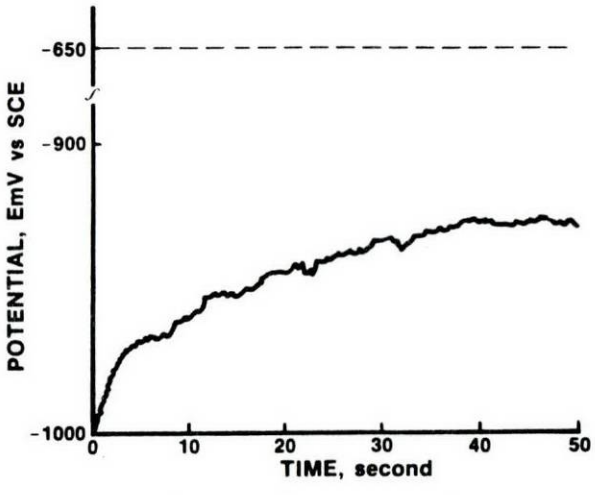

Figure 7. Potential-time curve for zinc foil immersion in EN plating bath.

(6) $Zn^{+2} + 2e^- = Zn^0, \quad E^0 = -0.763$

(7) $$E = E^0 - \frac{RT^\circ}{nF} \ln \frac{[Zn]}{[Zn^{+2}]}$$

or

(8) $$E = E^0 - \frac{RT^\circ}{nF} \ln [Zn] + \frac{RT^\circ}{nF} \ln [Zn^{+2}]$$

where,

E^0 = standard potential for the zinc reaction
R = gas constant
T' = temperature °K
F = Faraday's constant
n = number of electrons transferred
[Zn] = activity of zinc metal
$[Zn^{+2}]$ = activity of zinc ions

setting the activity of the solid zinc metal phase equal to unity, we obtain the equation (at 90° C),

(9) $E_{Zn} = -0.763 + 0.036 \log [Zn^{+2}]$

Initially, there will be very little zinc dissolved in the diffusion layer close to the metal substrate. In this case, $[Zn^{+2}] <<< 1$, giving a large negative value for $\log [Zn^{+2}]$. E_{Zn} will be substantially more negative than E^0, and a large thermodynamic driving force for zinc dissolution will exist.

As zinc dissolves into the diffusion layer, $[Zn^{+2}]$, the zinc activity will rise rapidly increasing the value of E_{Zn}. As E_{Zn} increases so will the mixed potential between zinc dissolution and nickel deposition, as seen in the potential-time curves of Figure 6. As E_{Zn} increases, it will attain and exceed the potential of the hypophosphite oxidation reaction. At this point, zinc reduction (deposition) will occur simultaneously with nickel deposition. Zinc will therefore be codeposited with nickel into the EN deposit forming the ZRZ.

Nickel deposited by replacement catalyzes the electroless or autocatalytic deposition reaction. When the deposition potential is reached, the EN reaction proceeds alone.

If the aluminum substrate is exposed to the EN plating solution as a result of zinc dissolution, a concurrent reaction, aluminum dissolution, occurs.

Aluminum dissolution: $Al = Al^{+3} + 3e^-, \quad E^0 = 1.66\ V$

Thermodynamically speaking, aluminum dissolution can trigger nickel and/or zinc immersion deposition at the sites where aluminum is dissolving. However, potential-time studies of the induction period for EN plating bare aluminum reveal that the potentials measured prior to attaining E_d are more positive than for zincated aluminum, as shown in Figure 8. If the zinc film was completely dissolved, exposing bare aluminum alloy to the EN solution, a sudden shift in potential to a value greater than E_d (>650 mV) should occur, followed by a rapid decrease to E_d. Since this does not happen, it must be assumed that the (E-t) curve of Figure 8 is due to the dissolution of the oxide coating on the aluminum or it reflects the change in E_{mix} for the hydrogen evolution-hypophosphite oxidation partial electrode processes that occur prior to metal deposition. Additionally, $|E^0_{Al}| > |E^0_{Zn}|$ so that (E-t) curves for Al dissolution should be in the same direction as the (E-t) curve for zinc dissolution. (E-t) curves for bare aluminum were similar to Figure 8 regardless of method of preparation of substrate. This implies that the oxide film reforms extremely fast.

The potential-time curve from the initial potential to E_d is smooth, i.e., the functional representation for the (E-t) curve is continuous.

The induction time for zinc dissolution/EN deposition varies with pH as shown in Figure 9. In the absence of EN bath stabilizers the functional relationship can be represented by the expression,

$$\left(\frac{\partial I_0}{\partial pH}\right)_{T^\circ,\ Al,\ Z,\ M} = f\ (pH)$$

where,

I_0 = induction time, no stabilizer case
T° = temperature
Al = aluminum alloy
Z = zincate solution
M = composition of plating bath

f(pH) is a continuously differentiable monotonic function of pH. When thiourea is added to the plating bath, the relationship is given by a straight line whose slope is,

$$\left(\frac{\partial I_s}{\partial pH}\right)_{T^\circ,\ Al,\ Z,\ M} = \text{constant}$$

I_s is the induction time for the stabilized case.

The importance of induction time studies will become apparent when the relationship between deposit stress, adhesion, and ZRZ are discussed.

Stress And Adhesion

In general, all electroless nickel deposits are in a state of internal stress. The stress may be compressive so that the deposit would like to expand parallel to the surface. In extreme cases of compressive stress, the deposit will buckle up on the substrate. Alternatively, the deposit may be in tensile stress, i.e., the coating would like to contract. The extremum of tensile stress is when stress forces are sufficiently large so that the elastic limit of the deposit is exceeded and it breaks up.

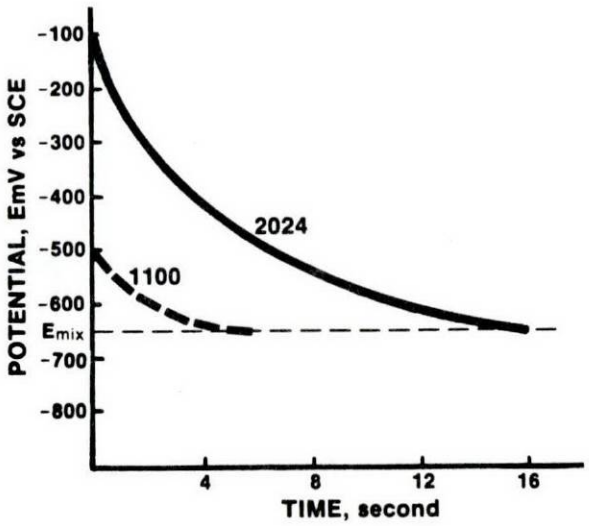

Figure 8. Potential-time curves for electroless nickel deposition on bare aluminum alloys.

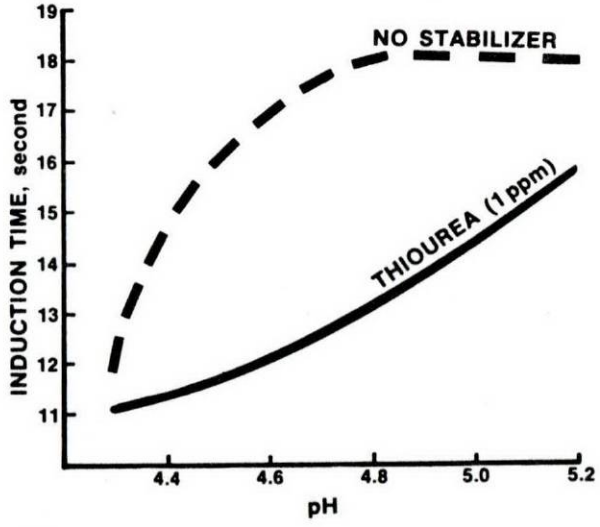

Figure 9. Effect of bath pH on induction time (zincate solution B).

Movement of the deposit relative to the substrate (loss of adhesion) will take place only if the adhesive bond between deposit and substrate is broken. When there is a loss of adhesion between the deposit and substrate, it is often found that the "free" deposit will curl up. This behavior indicates that the coating is stressed.

The internal stress in the EN deposit, σ_T, is the sum of two components, i.e.,

$$\sigma_T = \sigma_{intrinsic} + \sigma_{thermal}$$

The intrinsic stress, σ_i, results from crystal and lattice growth defects introduced into the deposit during deposition. The expression used to calculate σ_i was given in equation (5).

When the coefficients of thermal expansion of the EN deposit, α_d, and the substrate, α_s, are different, cooling the system produces the second component of σ_T, the thermal stress σ_H. This necessitates the addition of a correction term to equation (5) to account for the difference in the expansion coefficients, as follows:

$$(10) \qquad \sigma_H = (\alpha_d - \sigma_s)\left[\frac{E(\Delta\tau)\ (T + t)}{(T + t)^2 + 3Tt}\right]$$

where $\Delta\tau$ is the difference between the plating bath temperature and room temperature.

The type and magnitude of the thermal stress contribution depends on the term $(\alpha_d - \alpha_s)$. When $(\alpha_d - \alpha_s)<0$, the contribution is compressive; if $(\alpha_d - \alpha_s)>0$, the contribution is tensile in nature. When electroless nickel plating aluminum, $\alpha_s>\alpha_d$, $(\alpha_d - \alpha_s)<0$ and σ_H is compressive.

Relationships such as stress versus pH of EN bath, stress versus phosphorus content of deposit, and plating bath pH versus P content of deposit have been well studied, particularly when EN plating ferrous alloy substrates. Parker and Shah[12] reported stress data for EN plating several metal alloys including beryllium and aluminum. Their results are given for measurements taken at room temperature.

The effect of pH on the stress of Ni-P films (deposited on aluminum from the experimental plating bath) is shown in Figure 10. The intrinsic stress of EN deposits on aluminum varies with pH in a similar fashion to σ_i for deposits on ferrous alloys. That is, when the pH of the plating bath is greater than 4.7, σ_i is tensile; for pH values less than 4.7, σ_i is compressive. To illustrate this fact, σ_{i304} is included in Figure 10. It can be assumed

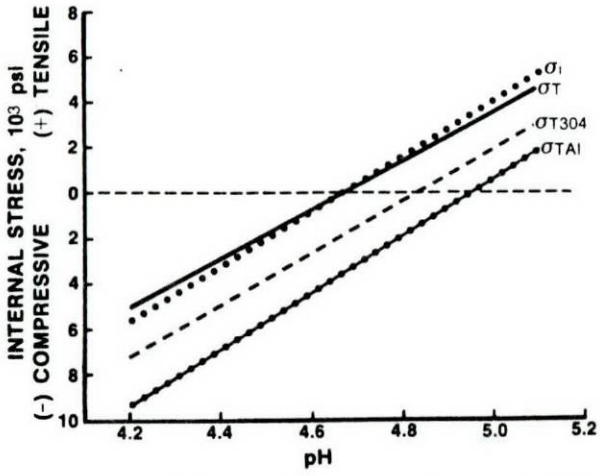

Figure 10. Effect of pH on stress of EN deposits.

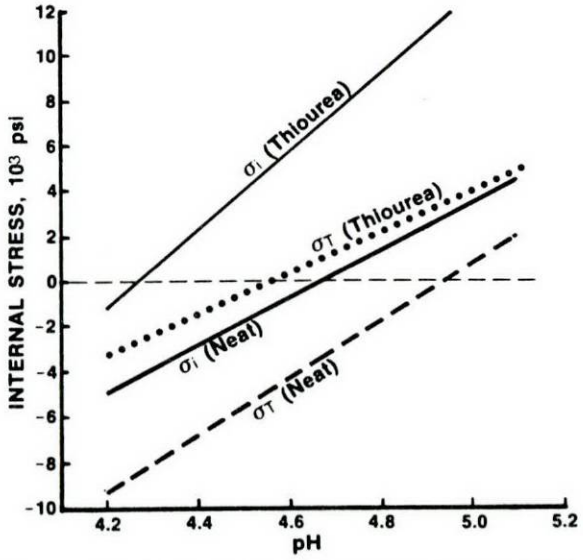

Figure 11. Effect of stabilizer on stress of EN deposits as a function of pH.

that the substrate has only second-order effects on the intrinsic stress of the deposit. The curve depicting the variation of the total (residual) stress lies in the compressive region for all values of pH studied. The effect of the difference in thermal expansion coefficients is shown by comparing the two curves σ_{TAl} (aluminum) and σ_{T304} (304 stainless steel). The expansion coefficients have a first-order effect on σ_T.

The addition of a stabilizer to the plating bath can influence changes in the stress of the resultant deposits. One ppm thiourea added to the EN plating bath shifts both σ_i and σ_T to more tensile values as shown in Figure 11. This increase in tensile stress can have a deleterious effect on adhesion.

With one exception, most investigators overlooked or ignored the effect of bath aging (regenerations) on the stress in EN deposits. By adding orthophosphite to several test solutions, Baldwin and Such[13] were able to simulate the accumulation of the product of hypophosphite oxidation that occurs during plating. They achieved a tensile stress of 17,000 psi at a phosphite concentration of 120 g/L. The EN film was deposited on a copper-plated steel substrate. Performing similar experiments in this laboratory with aluminum substrates, the intrinsic stress was increased to 15,000 psi tensile (Figure 12). Equivalent results were obtained by actually regenerating the bath a sufficient number of cycles to accumulate 160 g/L orthophosphite (curve 2 in Figure 12).

Finally, stress can be affected by changes in the concentration of complexing agent in the plating bath, as illustrated in Figure 13. At constant temperature, Ni^{+3}, $H_2PO_2^-$, and pH, σ_i is shifted to more compressive values when the concentration of lactate anion is increased from 1 to 6 times the molar concentration of nickel. It should be noted that increasing the concentration of complexing agent did not ameliorate the effect of the thiourea addition and return σ_i to lower stress values.

An absolutely necessary property of EN deposits is their adhesion to the substrate. The adhesion must be such that the deposit is not removed from the substrate by mechanical or thermal forces acting on the plated article. Adhesion can be defined as the force required to separate the deposit from the substrate. If the separation occurs at the interface, it is termed adhesive failure. If separation occurs within the substrate or within the deposit, it is termed cohesive failure.

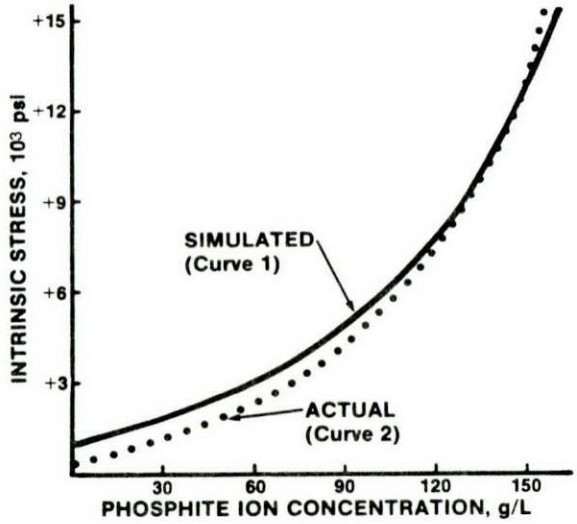

Figure 12. Variation of intrinsic stress with phosphite ion concentration.

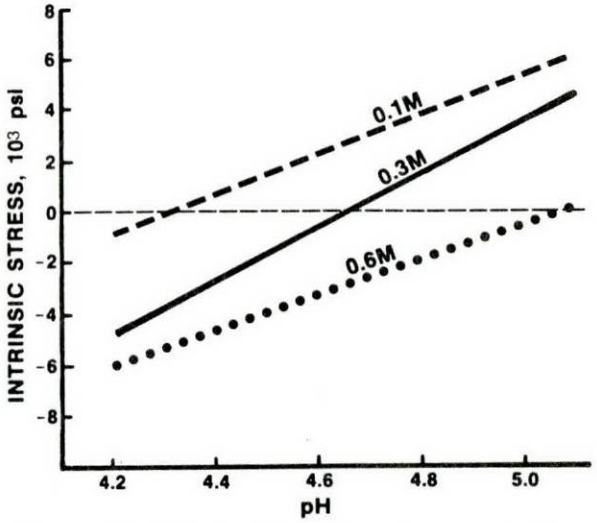

Figure 13. Effect of lactate anion concentration on intrinsic stress as a function of pH.

Auger spectrographic analysis of EN deposits that have separated from aluminum substrates indicate that either adhesive or cohesive failure can occur. Cohesive failure is predominant in the ZRZ. Analysis of both faces of the separation is required to determine which type of failure has occurred. This is represented schematically in Figure 14. Figure 14 shows that for adhesive failure the amount of zinc and nickel found in the substrate face is insignificant, while the ZRZ is intact on the deposit face only. For cohesive failure, remnants of the ZRZ is observed on the deposit face and the substrate face.

One method of determining adhesive failure is the visual observation of blister formation during plating. In this case, it was found that the intrinsic stress of the deposits exceeded (+) 12,000 psi tensile. Adhesive failure also occurred when the residual stress, σ_T, was greater in absolute value than (-) 10,000 psi compressive. Cracked deposits and blisters that form during salt spray testing are related, but not limited, to adhesive failure due to compressive stress.

Cohesive failure occurs to a lesser extent than adhesive failure. The conditions that lead to the formation of a very thick and brittle ZRZ, lead to cohesive failure. This type of failure occurs when the cohesion forces in the weak ZRZ are much less than the stress forces in that region. Under these conditions, fractures will occur in the ZRZ. Additionally, the binding forces between substrate and deposit (including ZRZ) must be greater than the internal stress forces causing the fractures in the ZRZ.

SUMMARY OF EXPERIMENTAL RESULTS

AES analysis at the interface of the aluminum substrate/Ni-P deposit (including ZRZ) shows that the zinc concentration in the ZRZ can assume two concentration profiles. The distribution of zinc in the ZRZ is shown in Figure 15. Curve 1 in Figure 15 shows the zinc concentration to have a Gaussian distribution over the thickness of the ZRZ. The zinc concentration gradient skewed toward the substrate is represented by curve 2. Adhesive and cohesive failure are related to the distribution profiles.

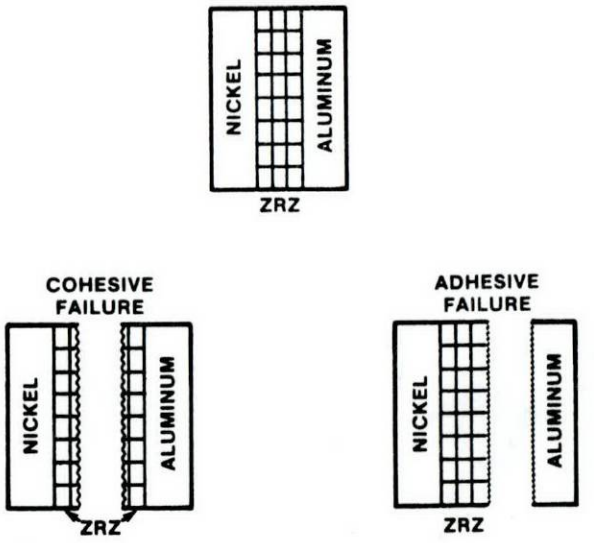

Figure 14. Schematic representation of adhesive and cohesive failure.

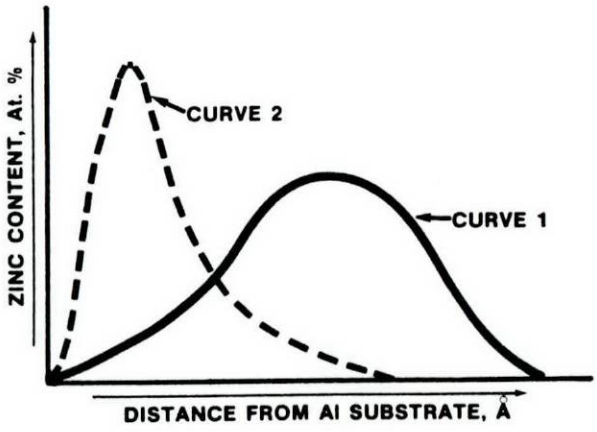

Figure 15. Zinc distribution in ZRZ.

Adhesive Failure

When the zinc distribution is diffuse and Gaussian in form, a high stress is required for adhesive failure. In this case, the intrinsic stress usually exceeds 15,000 psi tensile. Adhesive failure of Gaussian-distributed zinc occurs most frequently in ZRZ layers that are residue from zincate solution B.

The induction-time becomes important when considering adhesive failure of deposits plated on zincates from solutions A and C. The zinc films produced by zincate solutions A and C are much thinner than those from solution B. Small induction times result in higher zinc concentrations near the aluminum/ZRZ interface (curve 2, Figure 15). Factors that increase the rate of deposition, e.g., thiourea, and high pH, well exacerbate this condition. The type of stress required to cause adhesive failure in these cases could be either tensile or compressive. If the intrinsic stress is greater than 10 ksi tensile, failure will occur. If the intrinsic stress lies in the range 5 to 10 ksi, and the residual stress is near (−) 10 ksi compressive, adhesive failure will also result. Increasing the induction time by any method expands the ZRZ and causes the zinc concentration to be more diffuse in the ZRZ (Gaussian). A much greater stress force is required for failure.

Cohesive Failure

This type of failure occurred in ZRZ layers obtained from zincate solutions B and C. The zinc distribution in this case has the form given in Figure 16. A very brittle, high-zinc content layer with low tensile strength is formed in the ZRZ. When internal stress exceeds the tensile strength of this layer, separation occurs.

The conditions that lead to the type of cohesive failure discussed above usually occur when the EN plating solution has been regenerated several times, solution dragout has been excessive and the complexing agent concentration is low. The buffer capacity of the solution is lowered because of dragout and the pH drops rapidly during plating. Apparently, factors such as rate of zinc dissolution, induction time, pH, and rate of deposition are coupled in a manner that allows the formation of the brittle zinc layer in the ZRZ. These conditions also induce high internal stress in the deposit.

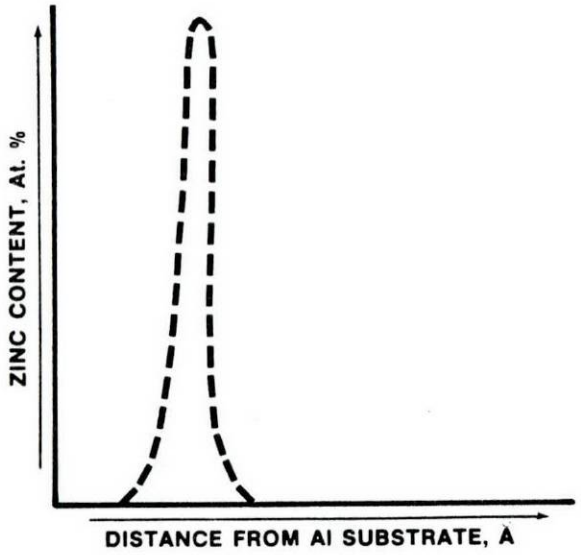

Figure 16. Zinc distribution in ZRZ (cohesive failure).

CONCLUSION

The type of zincate solution used in the EN plating of aluminum has a pronounced effect on the subsequent adhesion of the EN deposit. Each zincate deposits a zinc film of characteristic thickness and composition. These films lead to the formation of a zinc rich zone in the EN deposit next to the aluminum substrate. The zincate of choice is one that ultimately yields the thinnest ZRZ.

The distribution of zinc in the ZRZ is influenced by the chemistry of the EN plating bath. EN solutions that lead to diffuse zinc distribution are preferred. Stabilizers that shorten induction time should be avoided if possible.

Plating bath conditions that yield deposits of high stress are to be avoided. The internal stress can be monitored using the Brenner-Senderoff Contractometer. This allows for the determination of the intrinsic and residual stresses.

REFERENCES

1. E. H. Hewitson, U.S. Patent 1,627,900 (1927)
2. J. Korpium, U.S. Patent 2,142,564 (1939)
3. L. Perner, U.S. Patent 2,297,241 (1942)
4. E. B. Saubestre and J. L. Morica, *Plating*, **53**, 899 (1966)
5. W. G. Zelley, *Journal Electrochemical Society*, **100**, 328 (1953)
6. F. Keller and W. G. Zelley, Ibid., **96**, 143 (1950)
7. S. J. Heiman, Ibid., **95**, 205 (1949)
8. A. W. Blackwood, E. F. Yarkosky, and J. F. Bongo, "Effects Of Surface Preparation On EN Plating On Aluminum", Proc. AES 68th Ann. Tech. Conf., **68**, (1981)
9. E. Yarkosky, M. Aleksinas, and A. Marczak, "Electroless Nickel Baths As A Factor In Producing Blisters On Aluminum", Proc. Am. Electroplating Society, **66**, Session P-4, (1979)
10. A. E. Wyszynski, Trans. of Institute of Metal Finishing, **45**, 147 (1967)
11. D. S. Lashmore, *Plating And Surface Finishing*, **67**, 37 (1980)
12. K. Parker and H. Shah, *Plating*, **61**, 58 (1974)
13. C. Baldwin and T. E. Such, Trans. of Institute of Metal Finishing, **46**, 73 (1968)

H-2

Electroless Plating
Session H

Performance of Electroless Deposits for EMI/RFI Shielding Applications

Gerald Krulik and John Waggoner
Enthone, Inc.
Bridgeview, IL

PERFORMANCE OF ELECTROLESS DEPOSITS FOR EMI/RFI SHIELDING

Gerald A. Krulik
Manager, Technical Service

John E. Waggoner
Marketing Specialist, Plating on Plastics

Enthone Incorporated
9809 Industrial Drive
Bridgeview, Illinois 60455

Environmental pollution of all types is a wide-spread modern problem. Government regulations have recently focused on a new area, electromagnetic interference due to uncontrolled emissions from electronic and electromagnetic devices. The Federal Communications Commission has set forth a series of regulations under Docket 20780 to control EMI and RFI, that is radio frequency interference.

The processes used for plating on plastics would seem to be a viable technique for RFI shielding. The basic techniques for applying electroless copper or any of the electroless nickels to plastics are well-known at the present time. Yet, little hard scientific data has appeared on the ability of these electroless coatings to work as EMI shielding. Likewise, there is little information on the corrosion resistance or general durability of such electroless coatings. The purpose of this paper is to show research results for various electroless nickels, electroless coppers and composite coatings, both for EMI shielding and for corrosion resistance. This information may help clarify some of the areas of uncertainty regarding the useability of POP for EMI/RFI shielding.

Why is plating on plastics a good choice for EMI/RFI shielding? One reason is that it will form a continuous film of uniform thickness over the whole surface of the part. This is very important in shielding because thin spots or scratches or uncoated areas would allow EMI radiation to leak out of the enclosure. Pure electroless coatings would seem to be the method of choice for these applications, rather than the traditional electroless followed by electrolytic coatings. The reason for this is that the electrolytic coatings often contribute to burn-off or thin spots in the low current density areas or at the contact points and give other problems. The work reported here has been done solely with pure electroless coatings of various kinds.

Some of the shielding possibilities include electroless copper, electroless nickel/phosphorus, electroless nickel/boron, electroless copper coated with immersion tin, electroless copper coated with a chromate or with an organic protective layer, and composites of electroless nickel and electroless copper. The coatings that we will discuss here are limited mainly to electroless copper, electroless nickel of various kinds, and composites of electroless nickel and electroless copper.

All test results reported here for EMI attenuation were obtained by the use of the transfer impedance method on special test panels. A series of test panels was prepared and analyzed for shielding efficiency as prepared. A subset of these panels was placed in salt-spray testing for 72 hours and then the panels were removed and again tested for RFI shielding efficiency. Another subset was placed in humidity testing for 336 hours and again at the conclusion of the test, the panels were tested for RFI shielding. Let's begin with the consideration of the RFI shielding efficiencies for various coatings. (Slide #1.) This slide shows the shielding efficiency in decibels upon the left versus the frequency in MHz or millions of cycles per second on the bottom. Frequency range covers that basically regulated by the FCC which is <.1 MHz to 1,000 MHz. This slide shows a series of test results for standard 7-8% nickel/phosphorus electroless coatings. Both sides of the test plaque were coated. The bottom line, number 1, corresponds to 7 mircoinches per side or 14 microinches total. As you can see, the shielding efficiency is very low, basically only suitable for electrostatic discharge applications. This had been expected from the very low conductivity of this thin film. Line number 2 shows a large jump up from about 15 to almost 40 decibels of shielding efficiency with a doubling of the electroless nickel thickness to 28 microinches or 14 microinches per side. Evidentally the thinner coating was not truly continuous because the resistivity of the coating dropped dramatically with the doubling of the thickness. Shielding efficiency is now basically minimal for many applications. Line 3 shows how the electroless nickel shielding efficiency increases when it is about doubled again to 48 microinches or 24 microinches per side, and finally line 4 shows another doubling of thickness to 94 microinches or 47 microinches per side. As you can see, there is a progressive increase in shielding efficiency with increasing thickness of electroless nickel.

Next (slide #2) shows the results for different types of electroless nickels. The top line shows the curve for 3% nickel phosphorus, with 32 microinches total thickness. This, having a higher conductivity than the nickel/boron, shows a higher shielding efficiency. The second line from the top shows 3% nickel/boron, 32 microinches total thicknesses. As you can

see, the nickel boron has slightly higher shielding efficiency than 6-7% phosphorus electroless nickel, which would be expected due to its higher conductivity. The third line down is for 6-7% nickel/phosphorus alloy, 28 microinches total thickness. The bottom curve shows 28 microinches of a 10-11% phosphorus high resistivity nickel/phosphorus coating. As you can see, the shielding efficiency is much lower than the rest. The basic general rule is that the higher the conductivity of the coating, the better the shielding efficiency.

This rule is borne out in the next slide, #3, which shows the effect of thicknesses for various pure electroless copper coatings. As you can see, a total thickness of 20 millionths of an inch of electroless copper has better shielding efficiency than 94 millionths of an inch of electroless nickel. As the thickness of the copper approximately doubles to 48 microinches and then again to 98 microinches, the shielding efficiency becomes very great. The shielding efficiences shown for the top line are greater than that required commercially for almost every device manufactured.

Slide #4 shows the effect of combining electroless copper and electroless nickel together for shielding applications. Three different coatings are incorporated in this figure. Line A is 7-8% nickel/phosphorus with a total thickness of 18 microinches (remember this is 9 microinches per side) over a total of 22 microinches of electroless copper. The second line, B, is 10-11% nickel/phosphorus, 18 microinches total, over 22 microinches of electroless copper. As you can see, the shielding efficiencies are essentially identical. The third slide shows 20 microinches of electroless copper total applied over 16 microinches of 7-8% nickel/phosphorus. Shielding efficiency is just slightly lower due to the lower copper thickness. What we have found is that the shielding efficiency of a composite coating, for all but the very thinnest layers of electroless copper, is dependent almost completely on the electroless copper. The electroless nickel used has almost no effect and I will go over this in a moment.

(Slide 5) Because the shielding efficiency is essentially independent of the electroless nickel's composition or thickness, it depends solely upon the electroless copper thickness. This slide shows the effect of different copper thicknesses versus shielding efficiency at the various frequencies. As you can see, electroless copper has excellent shielding efficiency at low frequencies and much better shielding efficiency at high frequencies. This is very important for several reasons actually. One of which is that most of the competitive methods such as nickel paints, copper paints, conductive plastics, and so forth would not even be shown in the graph because their shielding efficiencies at all wavelengths are at the low end or below the low end of that recorded here.

The second is that the FCC regulates different frequencies of radiation in different ways. Up through the 30 MHz range, the FCC regulates what is called conductive EMI/RFI. This is the radiation which escapes along power cords, through connectors and so forth. From 30 MHz to 1,000 MHz the FCC regulates transmitted EMI/RFI. This is the radiation which would escape through the plastic housing, through free space. It's very important that you have pore-free coating, a uniformly thick coating, and a high shielding efficiency, especially in the 30-1,000 MHz range. As you can see, electroless copper is outstanding in this frequency range.

(Slide #6) A little earlier I said that the composite of electroless nickel and electroless copper gets its shielding efficiency almost exclusively from the electroless copper. This is true because of the nature of the measurements that we make. Decibels of shielding efficiency is not a linear function as might be infered from the graph, but is a logrithmic function. Thus, there is a very large difference in actual shielding efficiency for each arithmatic difference of ten in dB of shielding efficiency. This slide shows the equation. If you do the calculations, you will see that if you take an electroless copper layer, which has 65 decibels of shielding efficiency, and overcoat with a layer of electroless nickel which by itself has 40 decibels of shielding efficiency, the total shielding efficiency of the coating is only 65.01 decibels. In other words, the 25 decibels difference in shielding efficiency between nickel and copper corresponds to a factor of several hundred difference in actual total shielding efficiency.

As we've seen, the relative shielding efficiency is different for electroless coppers and electroless nickels. Slide 7 shows relative conductivities of various metals based on copper being 1.0. On this same scale silver would rate 1.08 as it is more conductive than copper. On an equal thickness basis it would be a better shielding material. Electroless nickel is much less conductive than electroless copper. These conductivity figures are a very reliable guide to relative shielding efficensies of different coatings.

It is not only important to have a very good radio frequency interference shielding material on your plastic enclosure. It's also very important that this shielding material hold up over long periods of time. For example, if the coating would flake off or blister, there is a possibility that it could interfere with the electrical apparatus inside the case, perhaps short out some of the devices or circuits. Likewise, if you had a coating of RF shielding material only on one side of the plastics and part of it came off, you would now have a radio frequency leakage area. One of the advantages

of plating on plastics for RF shielding is that both sides of the part are plated. This provides a double protection against accidental scratches or blisters of any kind. Furthermore, the outside of most cabinets is painted for decorative reasons. This forms an additional layer of protection for the thin electroless layer.

The Underwriters Laboratory tests focus only on the adherence of any RF shielding coating to the substrate. Slide #8 shows the test methods employed by Underwriters Lab to qualify the coatings. As you can see, a modified thermocycle, a humidity, and an aging test are the test methods used.

In addition to mechanical adhesion though, there are some less obvious problems involved in RF shielding, one of which is the oxidation or degradation of the coating itself with time. There are two reasons for this being of grave importance. Oxidation may not seem too important if the part is painted, but not all of each part can be painted. All enclosures are made in two or more sections. The mating surfaces of each enclosure must be in electrical contact with each other. If these surfaces oxidize or degrade and form low conductivity or non-conductive paths, we now have what is known as a slot antenna. It is an interesting characteristic of radio frequency waves, that the amount of leakage through an aperture depends very little on the surface area of the hole but very strongly on the longest dimension of any such hole. Thus, a scratch one inch long will leak just about the same amount of radiation as a hole 1 inch in diameter. Likewise, if the whole perimeter of a box becomes non-conductive through oxidation of copper at the mating surfaces, then the whole box will radiate a very large amount of radiation.

One problem with using pure electroless copper is that copper is a very active metal and it oxidizes and breaks down fairly rapidly. We have run a series of tests to investigate the behavior of electroless copper and electroless nickel by themselves, along with combinations of nickel and copper in both salt-spray and humidity. Slide #9 shows the appearance of some of our duplicate series of test panels after 72 hours of salt-spray. Now it must be recognized that salt-spray is a very extreme test for a thin coating of 10-50 millionths of an inch. However, there is some applicability because perspiration and handling will deposit salt and cause coatings to degrade over time. Salt-spray can also be used as a rough guide to rank coatings.

Slide #9 shows the following:

Top row: electroless nickels

6-7% P 10-11% P 3% P 3% B

Second row: electroless coppers

As Is Anti-Tarnish Chromate

Third row: composites of nickel over copper

Cu + 6-7% P Cu + 10-11% P Cu + 3% P Cu + 3% B

Bottom row: composites of 6-7% nickel over copper

Cu + Ni + anti-tarnish Cu + Ni + chromate

10-11% P shows the least corrosion; 6-7% P panels are dark but not severely corroded. 3% P shows patches of corrosion with nickel salts and a few blisters. 3% B is very dark with small patchy areas of nickel eaten completely away.

All of the electroless copper coatings are badly corroded and pitted. Niether the anti-tarnish organic material nor the chromate gives any significant protection.

The composite coatings fared best. Large salt-spray performance differences are seen with the composites versus the plain electroless nickels. Niether the 6-7% phosphorus nor the 10-11% phosphorus nickels show any pitting. The high phosphorus coating is almost unchanged. The lower phosphorus coating has tarnished but has no pitting or green salts.

The 3% phosphorus panel shows erosion of the nickel in patches. The underlying copper, even though exposed, remains bright and shiny. This low phosphorus coating is more electrochemically active than the copper and is functioning as a sacrificial coating.

The 3% boron panel shows much green salt bleed thru from pores in the coating. Most of the panel is light in color and only slightly tarnished. The green salts are coming from the underlying copper. Here the Ni/B alloy is more noble than the copper and is accelerating, not retarding, corrosion at pits.

Slide #10 shows the shielding efficiency of electroless nickel on ABS after salt-spray exposure. This particular graph contrasts the results of a 6-7% phosphorus electroless nickel panel, total thickness 32 microinches versus the same panel after 72 hours salt-spray. You can see that the shielding efficiency has dropped in the low frequency range from about 40 decibels to about 30 decibels and in the higher frequency range, the difference increases to approximately 25 decibels. The actual loss in shielding efficiency by the electroless nickel is not too severe though. Again, this is very dependent

on the type of electroless nickel used. Higher phosphorus electroless nickels show less loss in shielding ability, and 3% phosphorus nickels show greater losses.

Slide #11 shows the results for electroless copper. There is much less difference after salt-spray exposure for the low frequency end, a difference of only about 8 decibels. However, by the time we get into the region of interest to the FCC for radiated RFI (>30 MHz), the difference becomes enormous, approximately 45 decibels. These figures illustrate again that electroless nickel is a fair coating by itself but not nearly as good as electroless copper. Unfortunately, electroless copper is very susceptible to corrosion and would not be suitable by itself in any application where a corrosive atmosphere would be expected to occur.

It is fortunate then that a composite of coating of electroless nickel on top of electroless copper offers the advantages of both coatings without any disadvantages. (Slide #12) This coating shows the same high shielding efficiency of electroless copper combined with the relatively good salt-spray resistance of electroless nickel. Again, the corrosion resistance of the electroless nickel coating over electroless copper varies with the type of electroless nickel, as I explained in my earlier slides. The slide here shows 6-8% phosphorus electroless nickel over standard electroless copper. As you can see, there is very little difference in shielding efficiency after salt-spray. What little difference there is is only in the high frequency and most of the differences can be related to experimental error. One thing that must be kept in mind is that even if the electroless nickel was almost completely corroded away, as long as the electroless copper layer was essentially untouched, there would be no difference in shielding efficiency. You must remember the figure I showed earlier on how the electroless copper layer itself dominates the shielding efficiency of this system.

Slide #13 shows the differences in the shielding efficiency of electroless nickel after 72 hours salt-spray at various frequency ranges. I have converted the decibels' difference into an arithmatic percentage drop based on the initial shielding efficiency. You can see that the drop in efficiency is anywhere from 90 to 99.75% based on the original shielding ability of the electroless nickel. You must recall, though, that this shielding efficiency, even after the drop, is still better than a number of competitive methods.

Slide #14 shows similar results for electroless copper. Here the efficiency drop is from 87% at low frequencies to 99.998% of the original value at higher frequencies. Again note that even at the higher frequencies, despite the percentage

decrease, the total shielding efficiency is still about equivalent to that of straight electroless nickel before salt-spray. One thing that operates very much in the favor of plated plastics in a test such as this is that most corrosion that takes place is on the upper-most portion of the test plaque. The lower-most portion of the test plaque is only slightly corroded and contributes the majority of the RF protection. These tests were run this way because this is indicative of what would happen in a real life situation - the outside of a cabinet containing electronics would be most exposed to corrosion.

Slide #15 shows the numerical differences for electroless nickel over electroless copper after salt-spray. Here the difference at the stated radio frequency intervals is only 2-3 decibels which is actually within experimental error. This difference translates into a 37-50% drop in actual shielding efficiency over the initial value. As you can see again, you must remember that the decibels of shielding efficiency is a logarithmic term.

Further data and discussions will cover the results for humidity testing.

The conclusions of this work are:

1. Plating on plastics is a very good method for RFI shielding applications.

2. Electroless copper is a much better shield than electroless nickel.

3. Electroless nickel offers better corrosion and oxidation resistance.

4. A composite coating of electroless nickel over electroless copper optimizes both RFI shielding efficiency and durability.

Acknowledgements

I want to thank all the people without whose help this project would have been impossible. This includes Carmine Nargi, Helen Craye, Jim Bongo, Juan Hajdu, and many others.

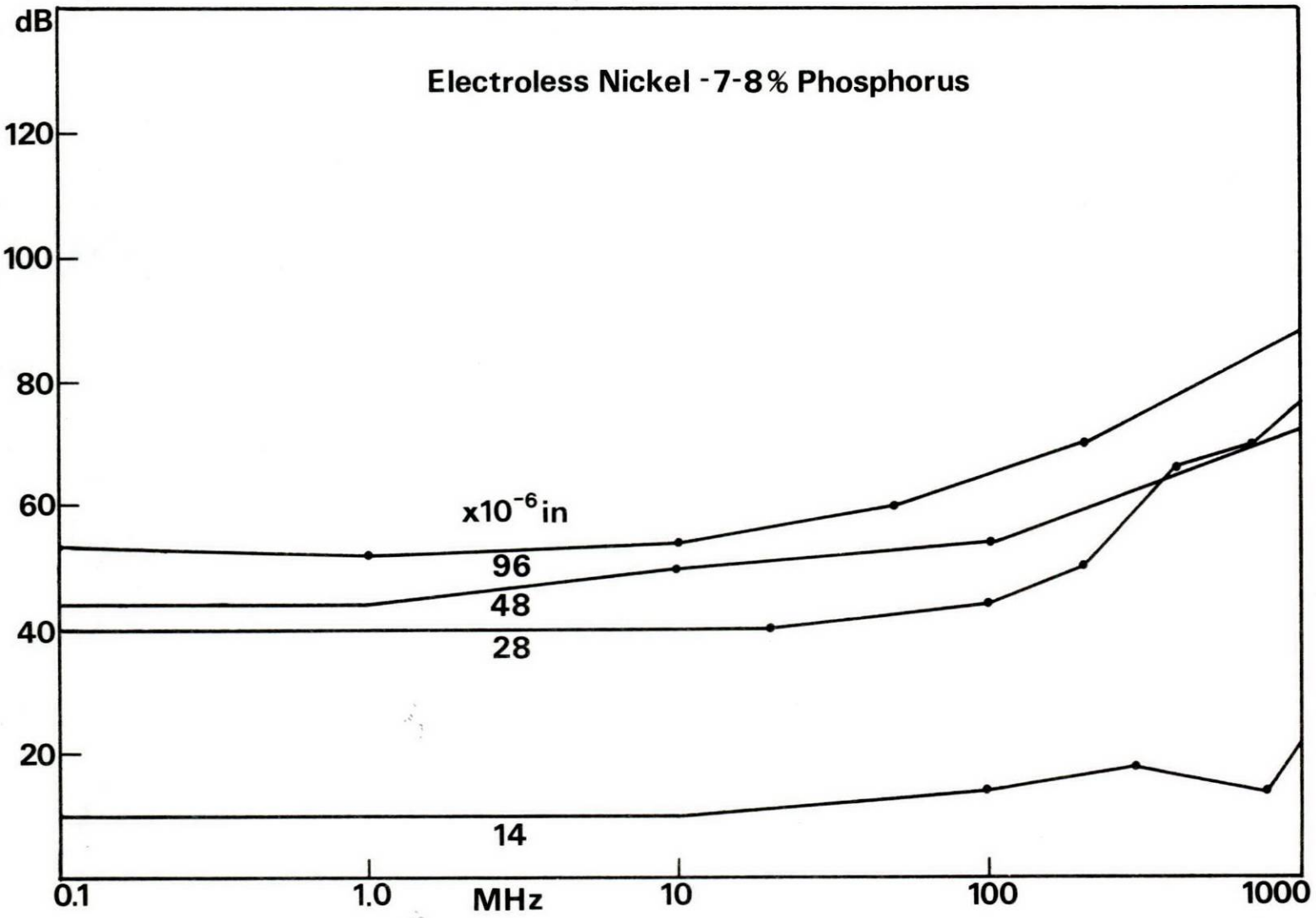

Fig. 1 Variation of Shielding Efficiency with Electroless Nickel Thickness

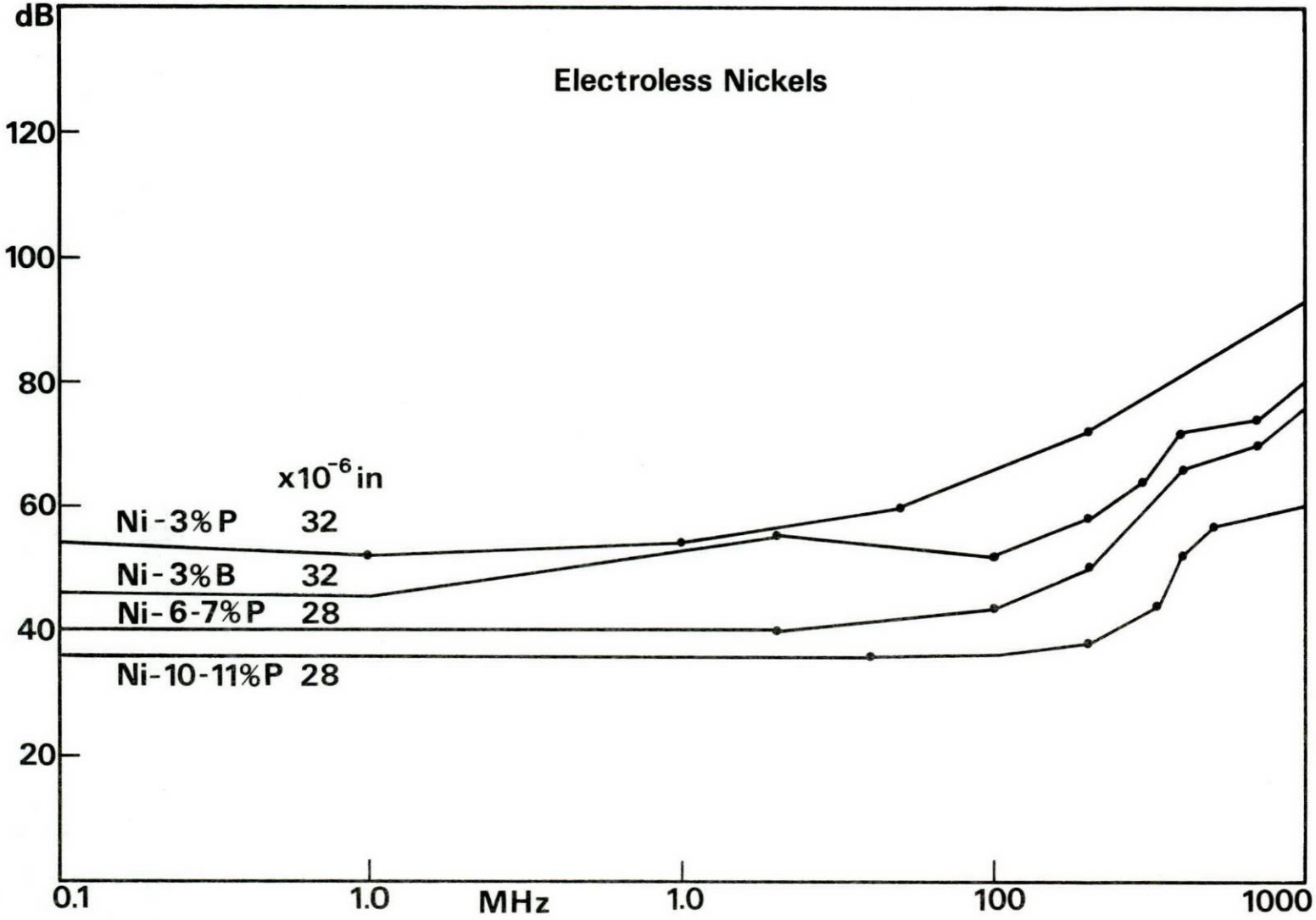

Fig. 2 Shielding Efficiency of Electroless Nickel Deposits

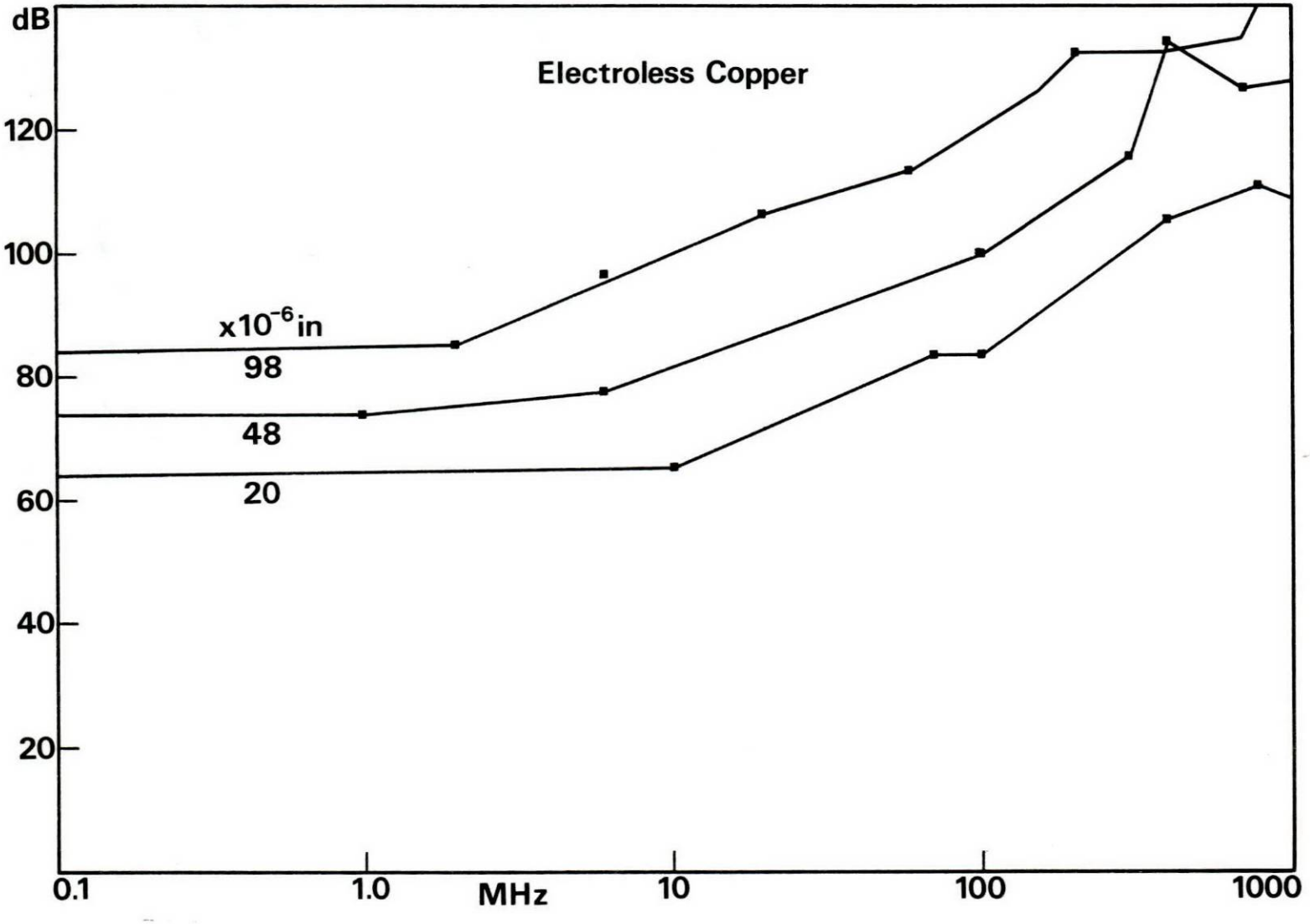

Fig. 3 Variation of Shielding Efficiency of Electroless Copper

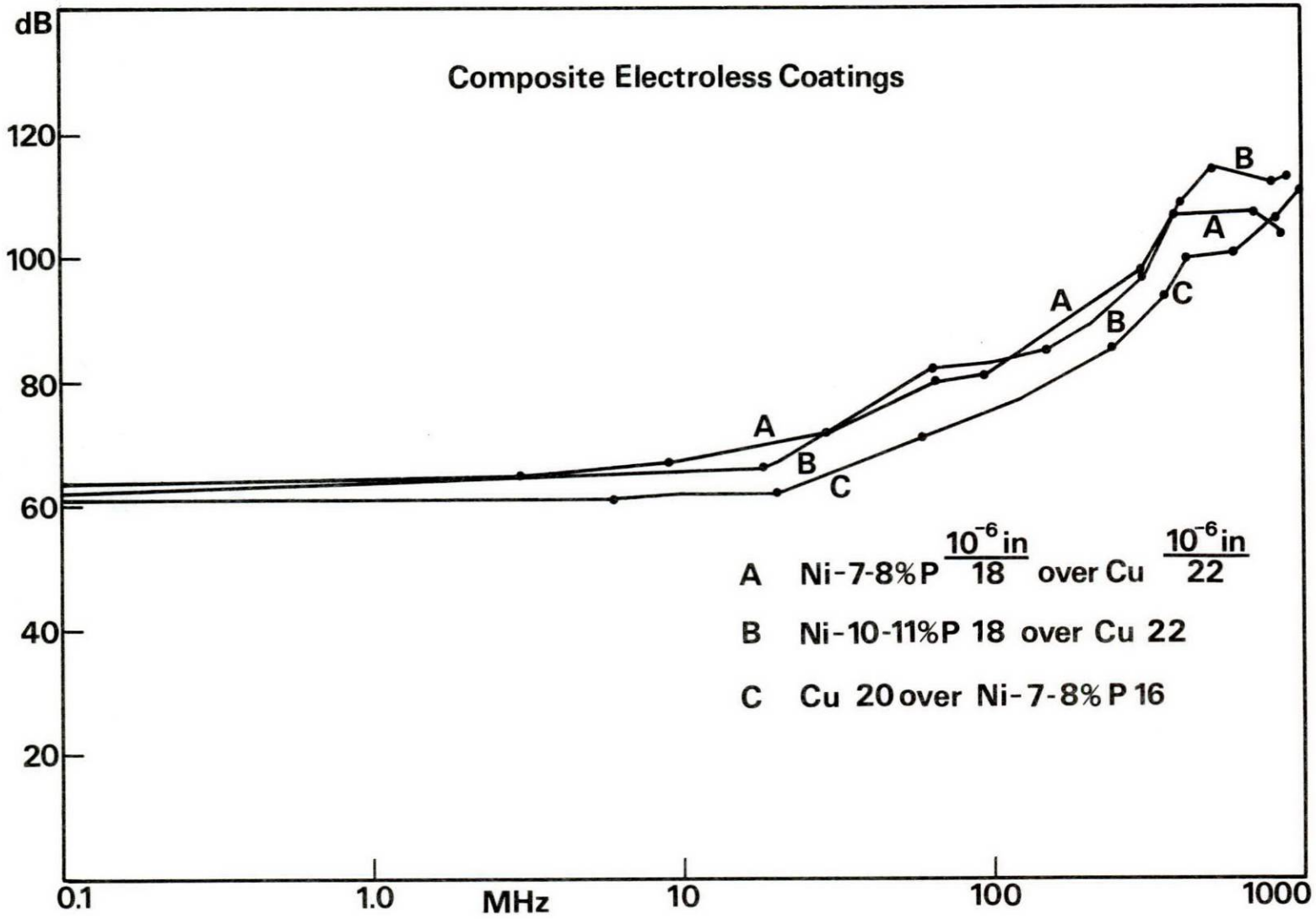

Fig. 4 Shielding Efficiency of Composite Electroless Coatings

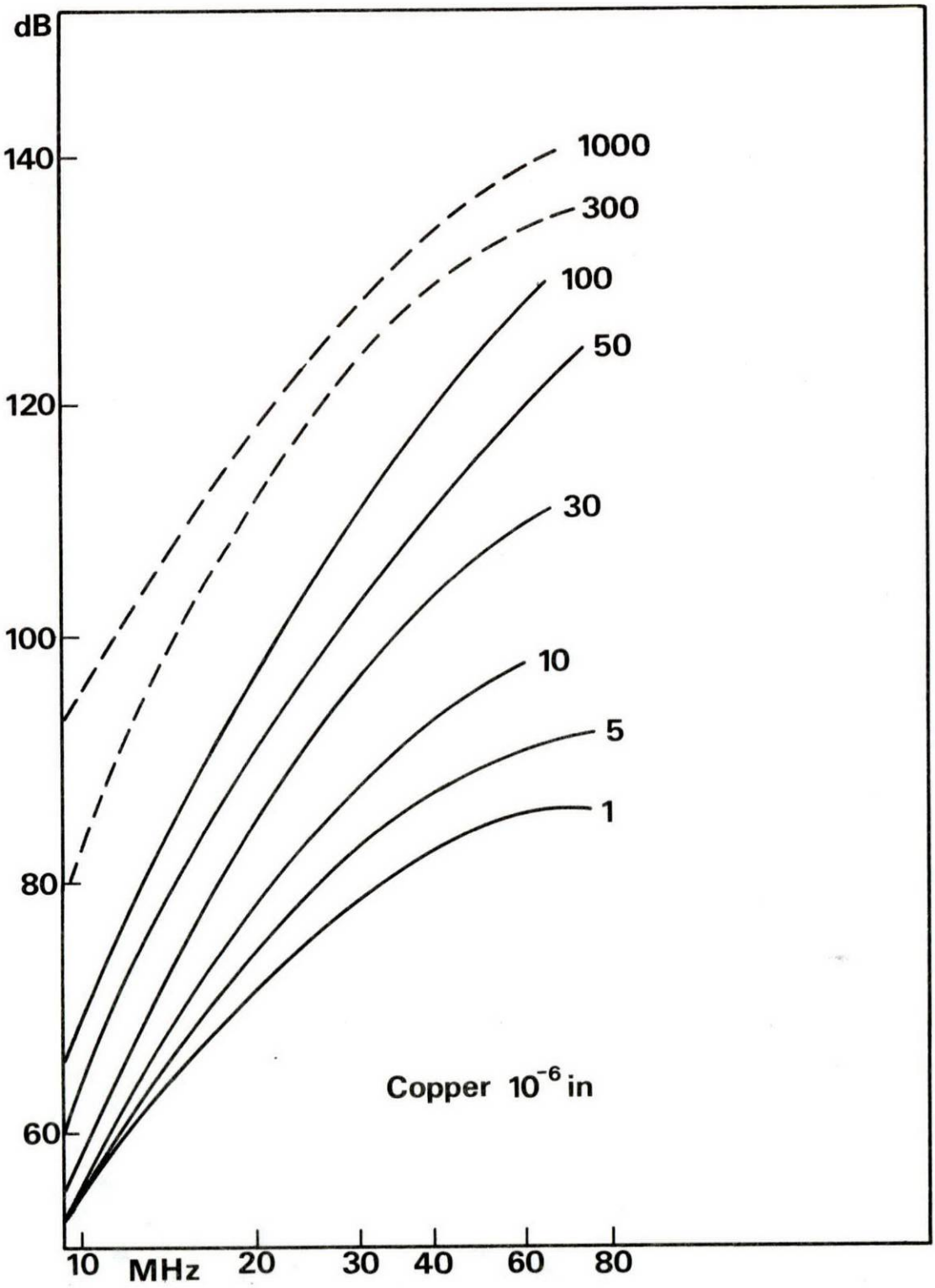

Fig. 5 Variation of Shielding Efficiency with Copper Thickness

FIGURE 6

$$dB = 10 \log \left(\frac{R_1}{R_2}\right)$$

If 65 dB electroless copper and
40 dB electroless nickel are combined,
the total shielding is 65.01 dB.

FIGURE 7

Relative Conductivity

Copper	1.0
Nickel	0.22
1% B/Ni	0.10
2.1% P/Ni	0.057
7% P/Ni	0.024

FIGURE 8

UL TESTS - RFI

ADHESION/CROSS HATCH

1. AS IS
2. HEAT AGED 85°C. 56 DAYS
3. HUMIDITY 90-95% RH 56 DAYS
4. THERMAL CYCLE 3X

R.T. - -29°C. - RT

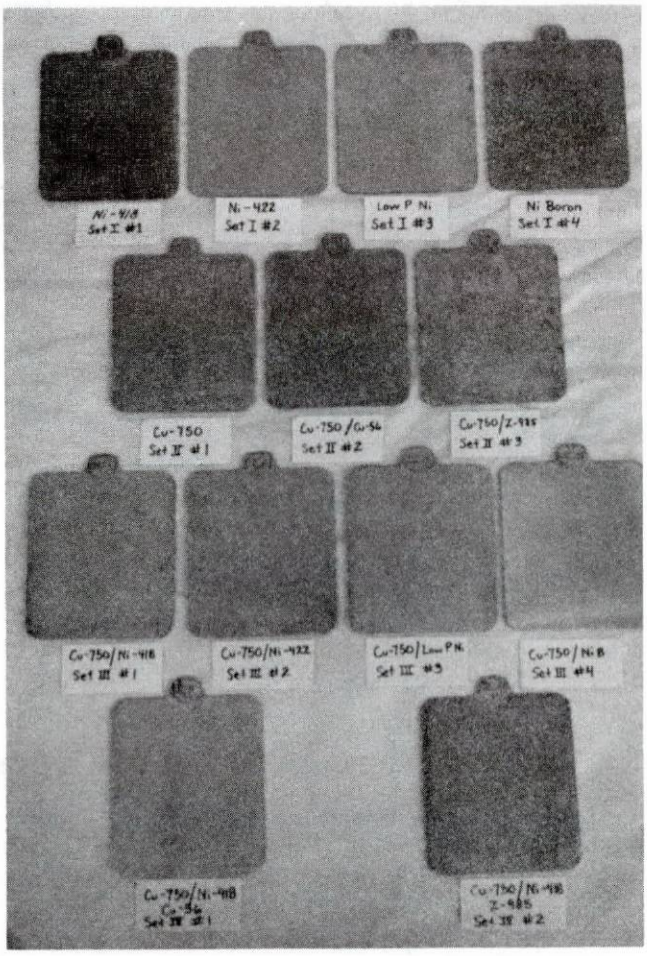

FIGURE 9

Salt-Spray Test Panels after 72 hours Exposure

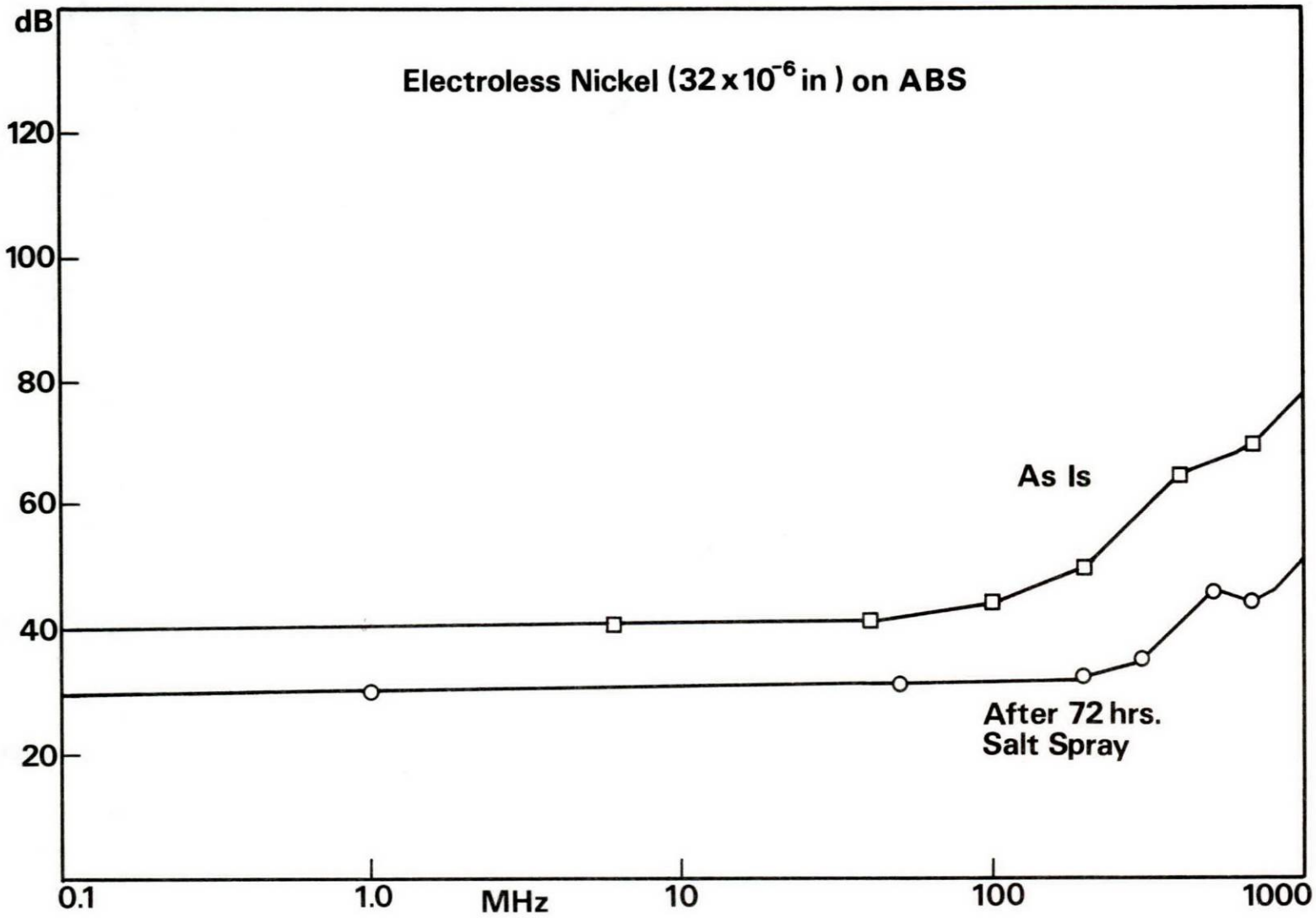

Fig. 10 Shielding Efficiency of Electroless Nickel after 72 hours Salt Spray Exposure

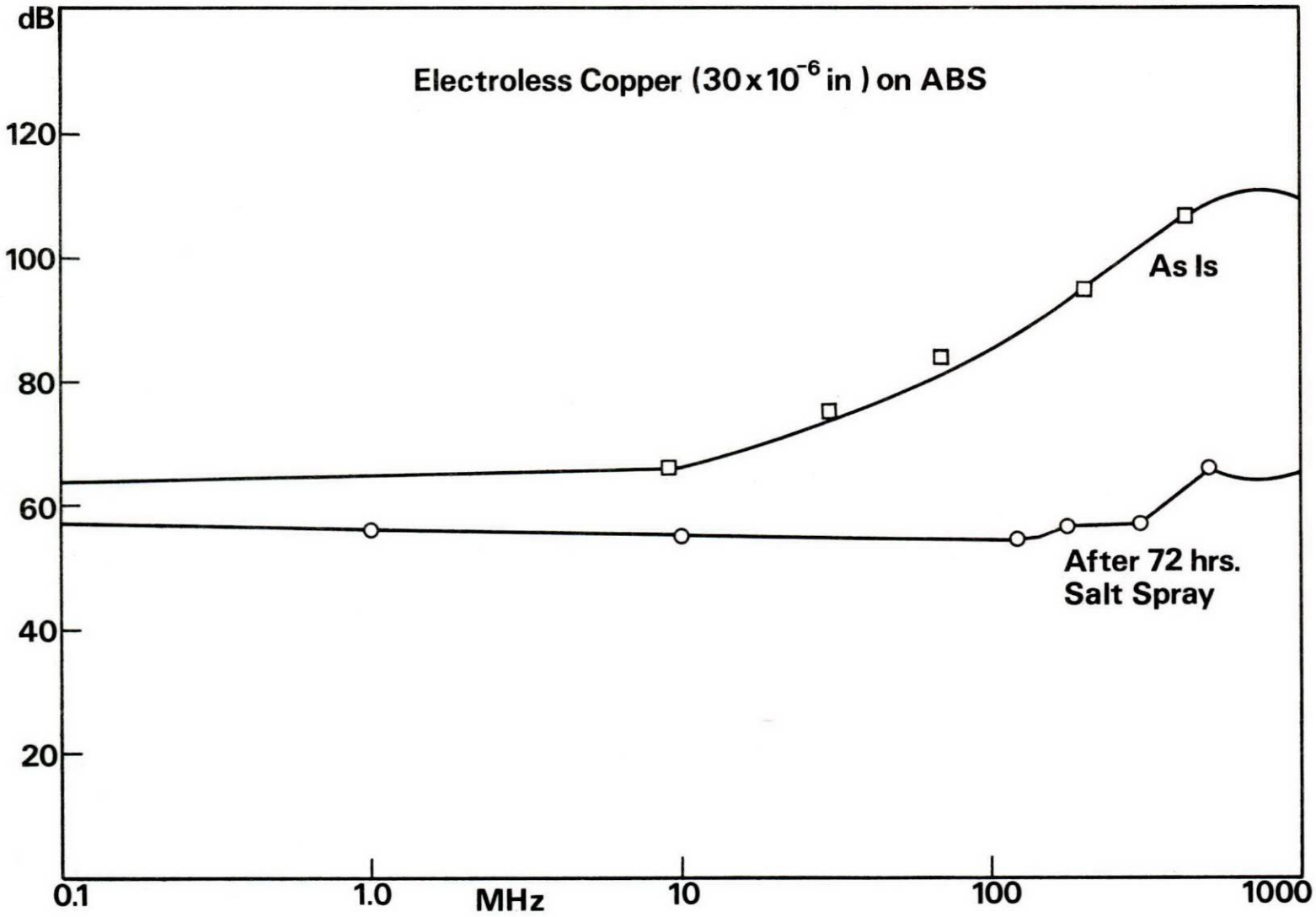

Fig. 11 Shielding Efficiency of Electroless Copper

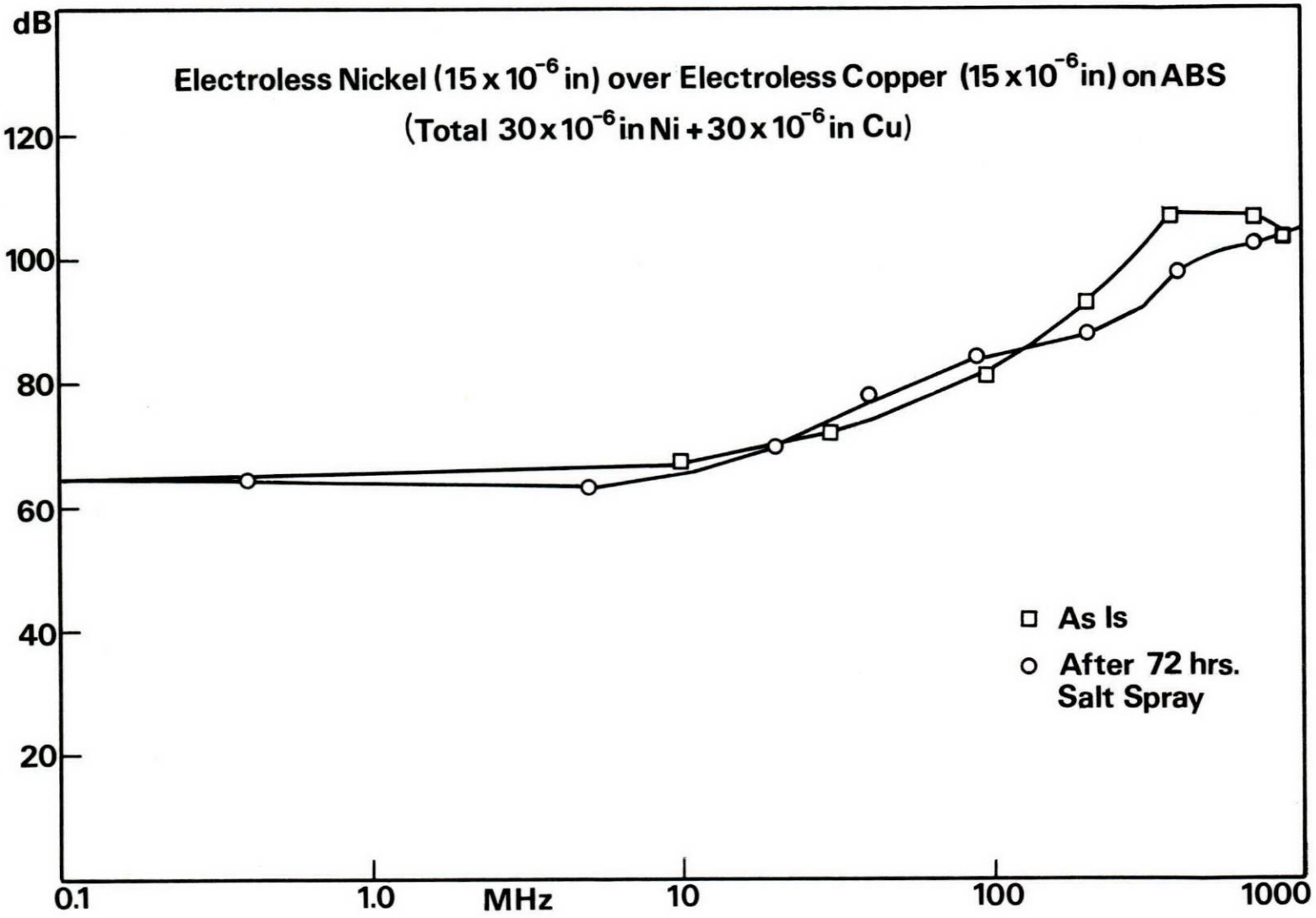

Fig. 12 Shielding Efficiency over Electroless Copper after 72 hours Salt Spray Exposure

FIGURE 13

Electroless Nickel

After 72 hrs Salt Spray

MHz	dB Difference	% Drop
1	-10	-90
10	-10	-90
100	-13	-95
800	-26	-99.75

FIGURE 14

Electroless Copper

After 72 hrs Salt Spray

MHz	dB Difference	% Drop
1	-9	-87.4
10	-11	-93
100	-33	-99.95
800	-47	-99.998

FIGURE 15

Electroless Nickel over Electroless Copper

After 72 hrs Salt Spray

MHz	dB Difference	% Drop
1	2	-37
10	2	-37
100	2	-37
800	3	-50

H-3

Electroless Plating Session H

Using Computer Technology in Electroless Nickel

Phillip D. Stapleton
Stapleton Company
Long Beach, CA

USING COMPUTER TECHNOLOGY IN ELECTROLESS NICKEL

Phillip D. Stapleton
Stapleton Company
1350 W. 12th Street
Long Beach, CA 90813

Abstract

Computers in the metal finishing industry can improve control of operations, automate repetitive operations, and provide for an orderly systematic growth. An application like operating an electroless nickel process can serve as an example of how a computer could be incorporated into metal finishing. This article covers the formulation of an electroless nickel data base, use of auto-analyzer on electroless nickel solutions, and overall design of system.

Computers are playing an ever-increasing role in improving the efficiency of metal finishing operations. Computers are also in the midst of a quantum transformation which will carry through into the 21st century. A typical piece of hardware like the 1.2 megabyte double-density floppy disc has been replaced by a 5 megabyte hard disc, which in turn will be replaced by a 50 megabyte and a 500 megabyte disc within five years. Other new technologies include Virtural Operating Systems (a type of unrestricted memory addressing) and light-powered computers. These advances will bring many new applications for computers and will force many of us to be directly involved in using these tools if we are to remain competitive within our respective fields.

The major reasons for using a computer in the plating industry and improve the efficiency are:

1. Improve control of operations
2. Automate repetitive operations
3. Provide for orderly systematic growth

We will discuss each of these reasons in reverse order.

Whenever a computer system is contemplated, several critical steps in organization are required. These steps involve describing the information required, all the input data necessary to compute the results, and how each item relates to one another. To accomplish this organization of each task, large flow charts may be developed which can trace how bits of information are processed. Using item list and flow charts, you will be able to visualize how you are processing information and how a computer might do it.

An example of this process can be seen in developing a program to monitor an electroless nickel process. In an electroless nickel process there are several factors and bits of information which are available and would be nice to know. If these were placed on a chart, they might look like Figure 1.

As all this information is assimilated into the computer system, reports may be generated which will provide management with the tools to operate efficiently. As you can see, a manually kept record would be awesome with 200 lots in process, while a mini-computer system would have no problem keeping up.

The important factor at this point is to understand that before you get a computer you must have a very complete definition of exactly what you need. Failure to identify a particular bit of information may cause thousands of dollars in software changes.

Another important consideration when organizing a system is how the reports are going to be used. In our operation we generate several monthly summary reports (Product Sales Analysis by Lot, etc...) which are important when the need arises to analyze some events. We seldom use these reports, however, because of the great amount of detailed information they include and limited requirements. This information will be stored in the computer data base in the future and seldom printed but available for query. In this example from Figure 1, the dates and times in and out would never need to be printed unless a rime study was undertaken.

To collect this information by manual means and compile it would be impossible, but with the use of data cap terminal or card reader it can all be automatic. To review all of this information would also be impossible, but yet the need does arise from time to time to analyze it. A sort and query program can be used to analyse large amounts of information quickly and provide the record of the event in question.

As you consider each task and what information is to be displayed and printed, logical CRT screens must be designed. With the use of sort and search software, information may be located and printed at will, providing for instantaneous review of any combination of data items. In addition, statistics on correlation of events can be made.

To establish these types of file systems (data bases), careful evaluation must be made of the software and hardware vendors you use. There are currently hundreds of data base systems available, many designed specifically for manufacturing and service industries.

By accomplishing these activities of organizing and evaluating the flow of information and capabilities of package software, a long-range plan can be proposed. This plan will provide you with the means to produce orderly systematic growth.

The second reason for using a computer is to automate repetitive operations. Some examples in a plating shop would include hoist control, inspection, billing, statements, quotations, analysis, automatic feed and word processing.

All of these functions can be integrated into most multi-terminal real time operating systems providing simultaneous processing of all functions.

If we continue the example of operating an electroless nickel system with a slight futuristic view, several interesting situations can develop. In this example, a host computer for a specific process is available which will coordinate user laboratory samples and user on-line solution analyses. The entire system uses phone and express mail communication. The system could provide electronic mail ordering and trouble shooting from the host computer as well as the standard business applications desired by most departments. All of the hardware exists today to accomplish building this system and will be available from several suppliers within a few years.

One feature which is unique to the metal finishing industry is the user on-line solution analyzer. This device which is available from several instrument companies provides for the separation and quantification of specific ions within the process. (See Figure 2) The Electroless Nickel Analyzer is able to analyze for the following:

Process pH
Process temperature
Nickel ion Ni++, Ni+++
Phosphorus PO2, PO3, PO4

Additives
- Brighteners
- Stabilizers
- Stress Reducers

Organic Solution Matrix

Anions Cl, NO3, NO2, SO4, SO2...

Trace elements Fe, Cd, Cu, Co, Cr, Pb, Sb...

As this information is produced at the users on-line analyzer, the coating alloy and solution performance can be tracked.

This continuous flow of information will be saved in the electroless nickel data base to be used later to generate certification, testing reports, and cost information. A general view of the hardware for such a system is shown in Figure 3.

This type of hardware system would depend on user samples being sent to the supplier labs and detailed analysis being coordinated with the user on-line analysis. With this situation, the system would be self-standardizing and maintenance would be kept to a minimum.

An additional feature of this computer system would be the ability of the purchaser or user of the coating to use the computer data base to assist in designing their parts by modeling corrosion performance and engineering properties. These could then be used to automatically adjust solution

operation to provide the specific properties desired and verify when the job is completed and what those properties should be. Additional testing by the supplier would then be used at periodic intervals to verify the accuracy of the on-line analyzer and modeling software. The information which is generated at the plating facility would be secured through several means, significantly reducing the chance to intercept valuable proprietary information by unauthorized persons.

These types of repetitive computer functions would relieve chemists and production people to be more creative and give them time to manage their departments far more effectively.

The third reason for computerization is to provide for the control of the operations. We have covered the organization and hardware and now come to the results of these efforts. For a manager to realize this phase, a tremendous effort will have had to be exercised in understanding the operation, flow of information, organization of software and hardware, training of operators, recovery of errors, and security. Each activity must be addressed and re-evaluated in order for the whole system to come together and the control of the particular operation be sound. Because Because this task is so large, it must be broken down into partitions which are manageable, and confidence must be developed each step of the way until the final goal is realized.

What is in store for the future in an information explosion. The ability of managers and technical persons to acquire, control, and disseminate this information will be critical to their success. What we have proposed here is being accomplished, and some are well on their way to using these powerful tools to make their operation run more efficiently and prepare for the future.

If you have throught about getting started and using a computer in your application, a suggestion would be to read as much as you can and talk to others who are doing what you want to do. Don't be a pioneer unless you are confident of success and remember that most applications have software which has already been written and may need little or no modification for your operation.

In this article we have attempted to point out some of the steps and goals necessary to address using computers in the metal finishing industry. The number of application possibilities are endless and care must be exercised to do those applications which will bring a savings and produce a benefit to your facility.

The management of an ever-increasing amount of detailed information will make the operation of metal finishing processes complicated. We trust that these thoughts and concepts will be of help in designing and planning your computer system.

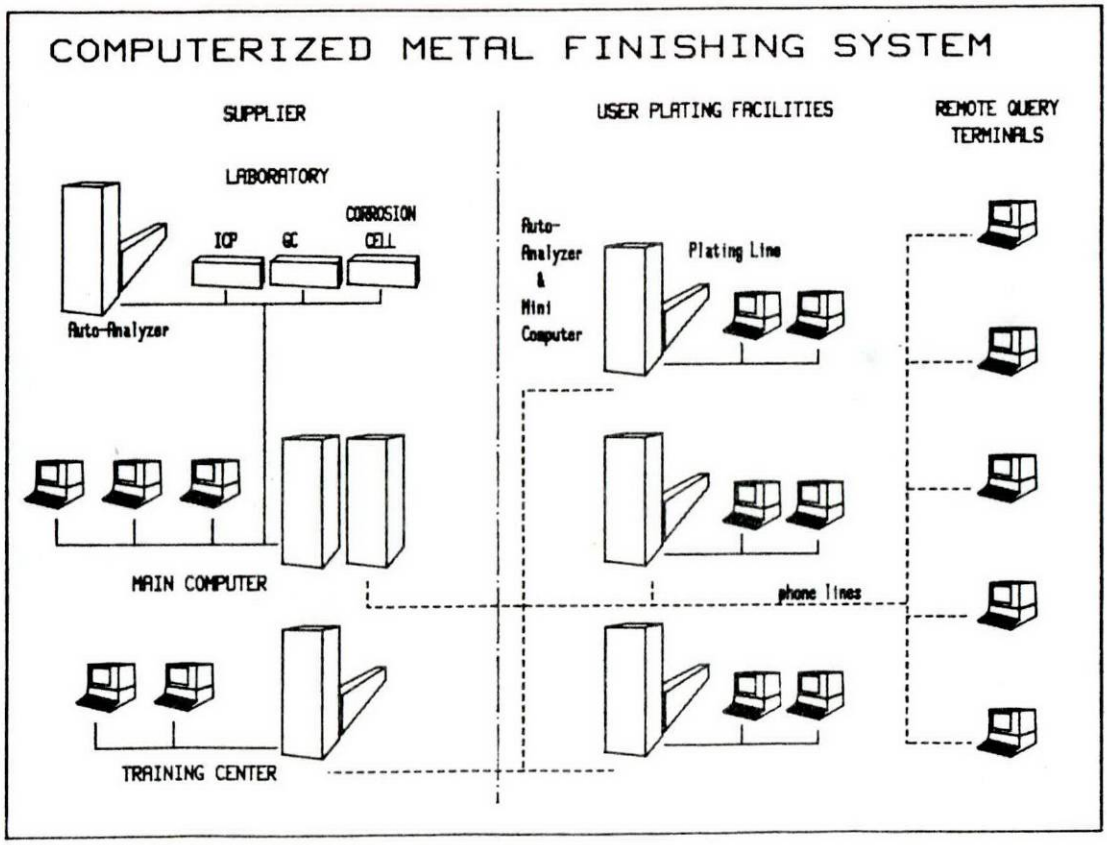
COMPUTERIZED METAL FINISHING SYSTEM
SUPPLIER
USER PLATING FACILITIES
REMOTE QUERY TERMINALS
LABORATORY
ICP
GC
CORROSION CELL
Auto-Analyzer
Auto-Analyzer & Mini Computer
Plating Line
MAIN COMPUTER
phone lines
TRAINING CENTER

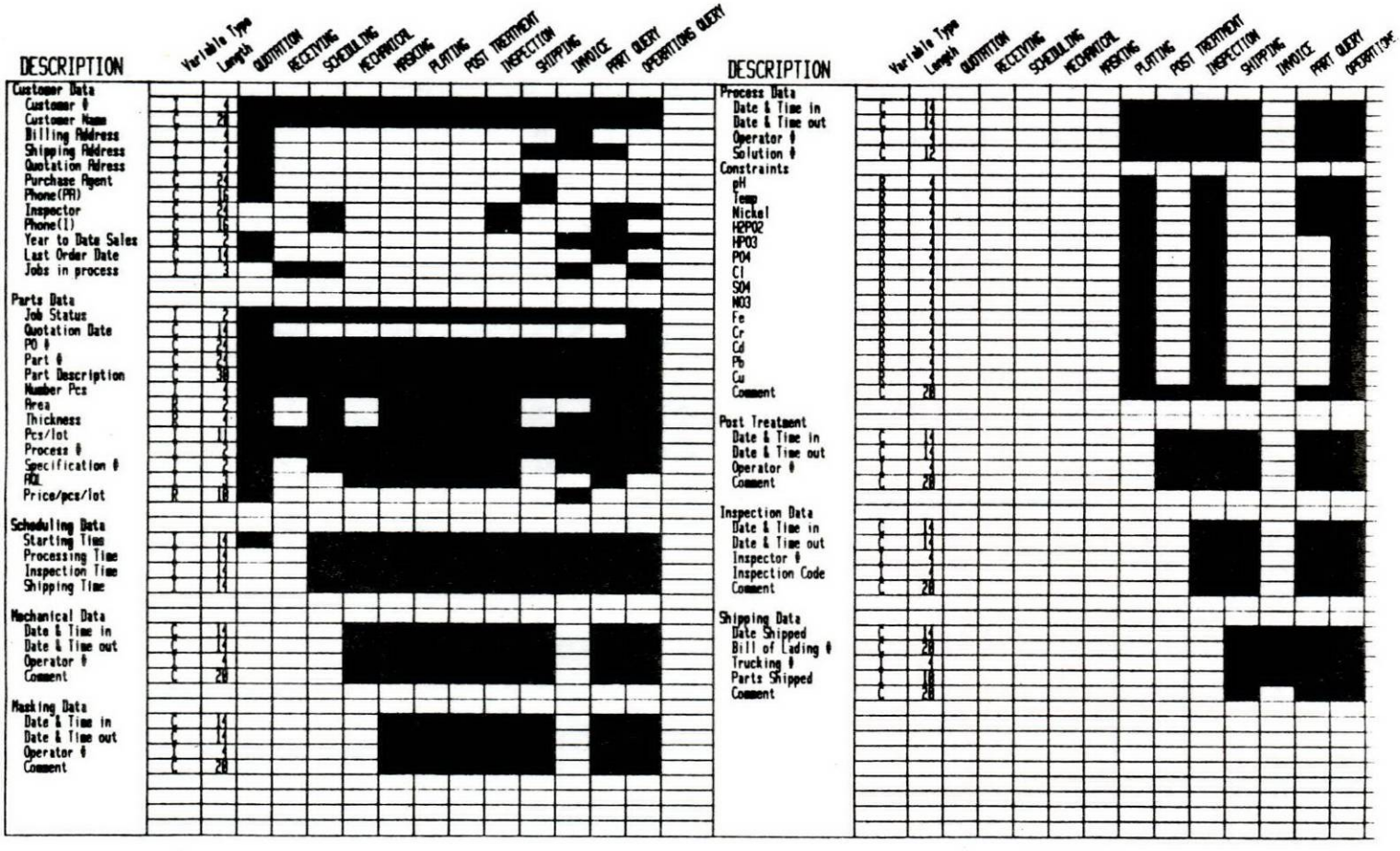
DESCRIPTION
Variable Type
Length
QUOTATION
RECEIVING
SCHEDULING
MECHANICAL
MASKING
PLATING
POST TREATMENT
INSPECTION
SHIPPING
INVOICE
PART QUERY
OPERATIONS QUERY
Customer Data
Customer #
Customer Name
Billing Address
Shipping Address
Quotation Adress
Purchase Agent
Phone(PA)
Inspector
Phone(I)
Year to Date Sales
Last Order Date
Jobs in process
Parts Data
Job Status
Quotation Date
PO #
Part #
Part Description
Number Pcs
Area
Thickness
Pcs/lot
Process #
Specification #
AQL
Price/pcs/lot
Scheduling Data
Starting Time
Processing Time
Inspection Time
Shipping Time
Mechanical Data
Date & Time in
Date & Time out
Operator #
Comment
Masking Data
Date & Time in
Date & Time out
Operator #
Comment
DESCRIPTION
Variable Type
Length
Process Data
Date & Time in
Date & Time out
Operator #
Solution #
Constraints
pH
Temp
Nickel
H2PO2
HPO3
PO4
Cl
SO4
NO3
Fe
Cr
Cd
Pb
Cu
Comment
Post Treatment
Date & Time in
Date & Time out
Operator #
Comment
Inspection Data
Date & Time in
Date & Time out
Inspector #
Inspection Code
Comment
Shipping Data
Date Shipped
Bill of Lading #
Trucking #
Parts Shipped
Comment

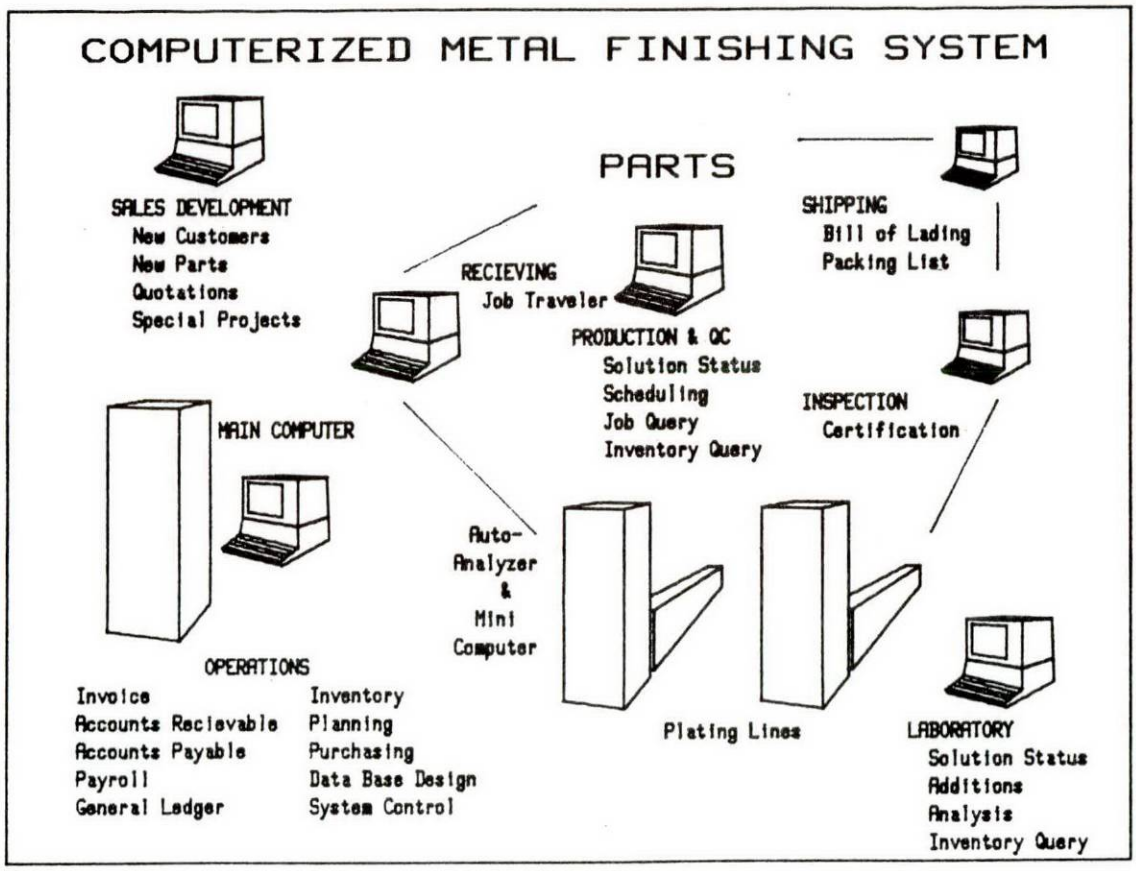
COMPUTERIZED METAL FINISHING SYSTEM
PARTS
SALES DEVELOPMENT
New Customers
New Parts
Quotations
Special Projects
RECIEVING
Job Traveler
SHIPPING
Bill of Lading
Packing List
PRODUCTION & QC
Solution Status
Scheduling
Job Query
Inventory Query
INSPECTION
Certification
MAIN COMPUTER
Auto-
Analyzer
&
Mini
Computer
OPERATIONS
Invoice
Accounts Recievable
Accounts Payable
Payroll
General Ledger
Inventory
Planning
Purchasing
Data Base Design
System Control
Plating Lines
LABORATORY
Solution Status
Additions
Analysis
Inventory Query

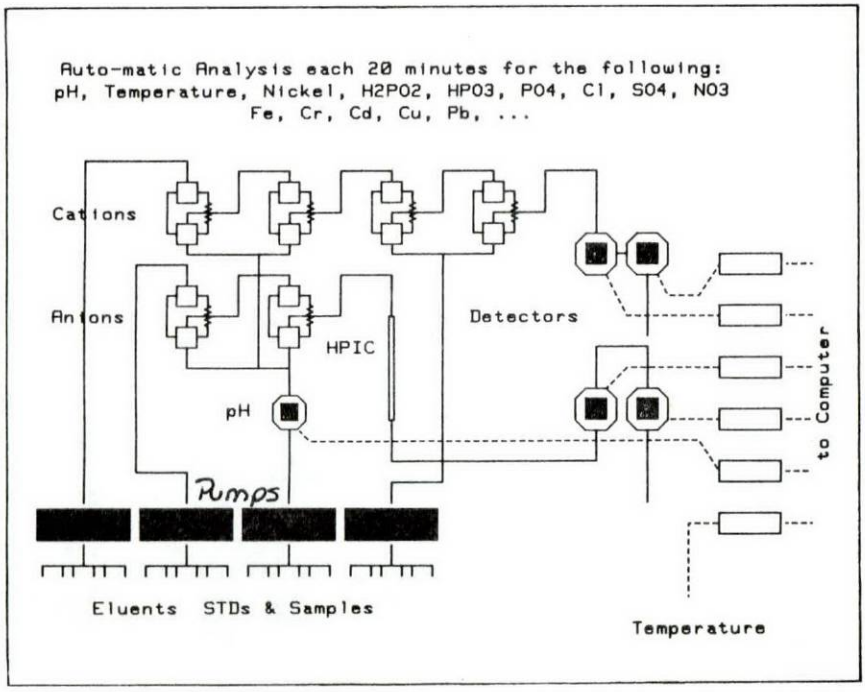
Auto-matic Analysis each 20 minutes for the following:
pH, Temperature, Nickel, H2PO2, HPO3, PO4, Cl, SO4, NO3
Fe, Cr, Cd, Cu, Pb, ...
Cations
Anions
HPIC
pH
Pumps
Detectors
to Computer
Eluents STDs & Samples
Temperature

H-4

Electroless Plating
Session H

Electroless Gold

Dr. Raichur Narayan
TRW Connectors
Elk Grove Village, IL

ELECTROLESS GOLD

Dr. Raichur Narayan
Manager R & D Plating Lab
TRW Connector Division
1500 Morse Avenue
Elk Grove Village, IL 60007

Abstract

This paper describes a new non-cyanide electroless gold solution which is capable of depositing 3-4 microinches per minute of 24 karat gold on electroless nickel plated surfaces and 2-3 microinches per minute on immersion gold plated surfaces. The solution is superbly stable over very long periods of time, even at 200°F. Physical characteristics and kinetics are discussed, but not the chemical composition.

Introduction

Aside from some old formulations (1) which were called electroless while they were actually immersion baths, there have been, indeed, no real autocatalytic gold plating processes developed except two formulations (2, 3) developed by Sel-Rex and Engelhard Industries, respectively. Like most electroless processes, these two suffer from instability and slowness, at operating temperatures typically ranging from 180°-200°F. Both formulations referred to (2, 3) are also cyanide based and use powerful reducing agents or reducing complexes. The so-called "high build" gold composition (2) builds only about 40 microinches per hour and the autocatalytic gold builds up to about 72 microinches per hour on Kovar substrates and even less on other metallic substrates. Similar results are obtained with the Engelhard process also (3). The process developed by this author deposits up to 300 microinches per hour on electroless nickel plated substrates and up to 150 microinches per hour on immersion gold plated substrates.

Experimental

After preliminary experiments showed that this particular bath is, indeed, electroless and after a definite bath composition was established, experiments were carried out to arrive at some usable parameters such as operating temperature range, concentration, pH and rates of deposition. It was found early that direct plating on copper and brass substrates could not be done from this bath. Thus all panels were plated with either electrolytic sulfamate nickel or electroless (hypophosphite) nickel or immersion gold.

2" X 1" panels of cadmium copper, phosphor bronze and 70-30 brass were prepared. All panels were degreased and cleaned in alkaline cleaner and neutralized with 20% sulfuric acid

before further treatments. In each category above, three different sets were prepared.

One die set was plated with sulfamate nickel (100-150 mins.), electroless nickel (100-150 mins.) and immersion gold (10 mins.). Panels in each such set were then coated with the new electroless gold for intervals of 5, 10, 20, 30 and 60 minutes. Each such experiment was carried out at 160°F and 180°F as typical operating temperatures.

Thickness Measurement

Thicknesses were measured by cross-section, Betascope and weight gain. To obtain the weight gain in milligrams, each panel was thoroughly dried to constant weight after the substrate plating (Ni or gold) and weighed after electroless plating after thorough drying to constant weight.

Results

A. Rate of Deposition

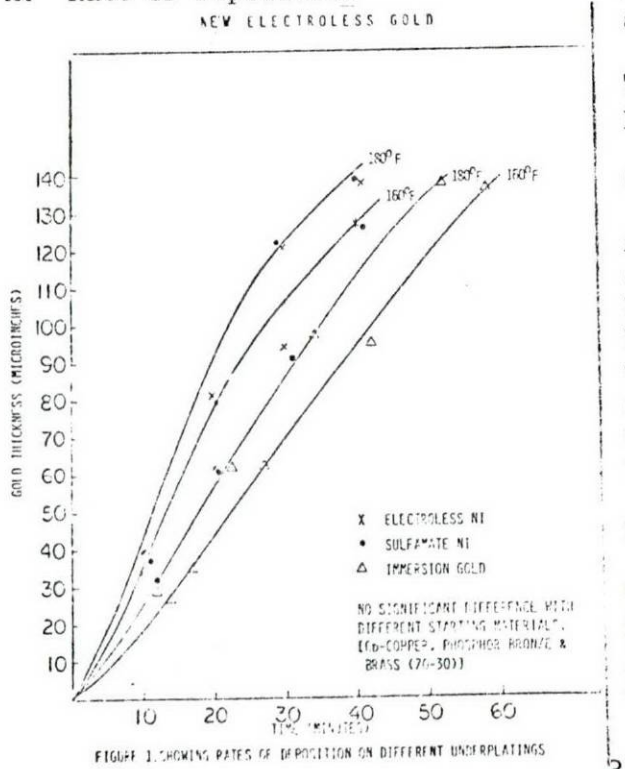

FIGURE 1 SHOWING RATES OF DEPOSITION ON DIFFERENT UNDERPLATINGS

Figure 1 shows a plot of thicknesses against time in minutes for each temperature, for each different substrate plated at the two different temperatures 160°F and 180°F. No elaborate studies were made at different pH values as there was no marked difference in pH value used (6-6.5). The figure shows clearly that the process is a true autocatalytic process with the rate leveling out exponentially with long times. It can be seen that the rate is close to an average of 4 microinches per minute on nickel plated panels and 2-3 microinches on immersion gold plated panels at 180°F and higher at 180°F.

B. Quality of Deposit

The thicknesses estimated from weight gain agreed almost exactly with those actually measured, thus showing that the deposits were of pure gold. EDAX analysis of the deposits also showed no evidence of contamination. The color was characteristic of pure gold and all deposits were smooth and bright, although no brightening agents are added to the bath.

The hardness of the gold on all panels was an average of 140 Knoop.

C. Adhesion

Adhesion checks were made by bending each panel through 180° and bending back 180°. Adhesion was found to be perfect on those panels where gold was deposited on electroless nickel and immersion gold. There was no adhesion on gold deposited on electroplated nickel.

D. Stability of Bath

There was no evidence of gold separating from the bath at boiling after 3-4 hours. There was no evidence of gold depositing on the walls of

the container (glass beaker or polypropylene). However, metallic particles such as nickel or gold introduced into the bath produced a slow build up on such nuclei.

E. Other Substrates

Unpassivated stainless steel, Kovar, metallized plastics and ceramics could all be plated without difficulty.

Discussion

The results of the experiments show clearly that an extremely efficient and practical autocatalytic gold process has been developed. The pH is near neutral. No filtration is necessary. Since the composition of the bath cannot be revealed, no discussion of the reduction mechanism can be given, suffice it to say that the system is not based on any known cyanide complexes. The system is patentable.

Conclusion

A highly stable, high speed and novel autocatalytic process has been developed. Its applications range from plating of electronic contacts of different shapes to plating of microelectronic circuits, including metallized ceramics. At the present time there is no method comparable available.

References

1. Y. Okinaka, "Gold Plating Technology", F. H. Reid and W. Goldie, Editors; Electrochemical Publications, 1974

2. K. Baker, U. S. Patent 1,193,823 (1970)

3. Alan Blair and Robert Stavitsky, "Electroless Gold", The First AES Electroless Plating Symposium, March 23-24, 1982, Sheraton, St. Louis, Missouri

Acknoledgements

The author wishes to thank TRW Connectors for permission to present this paper and also Mr. Richard Des•Champs for doing most of the experimental work.

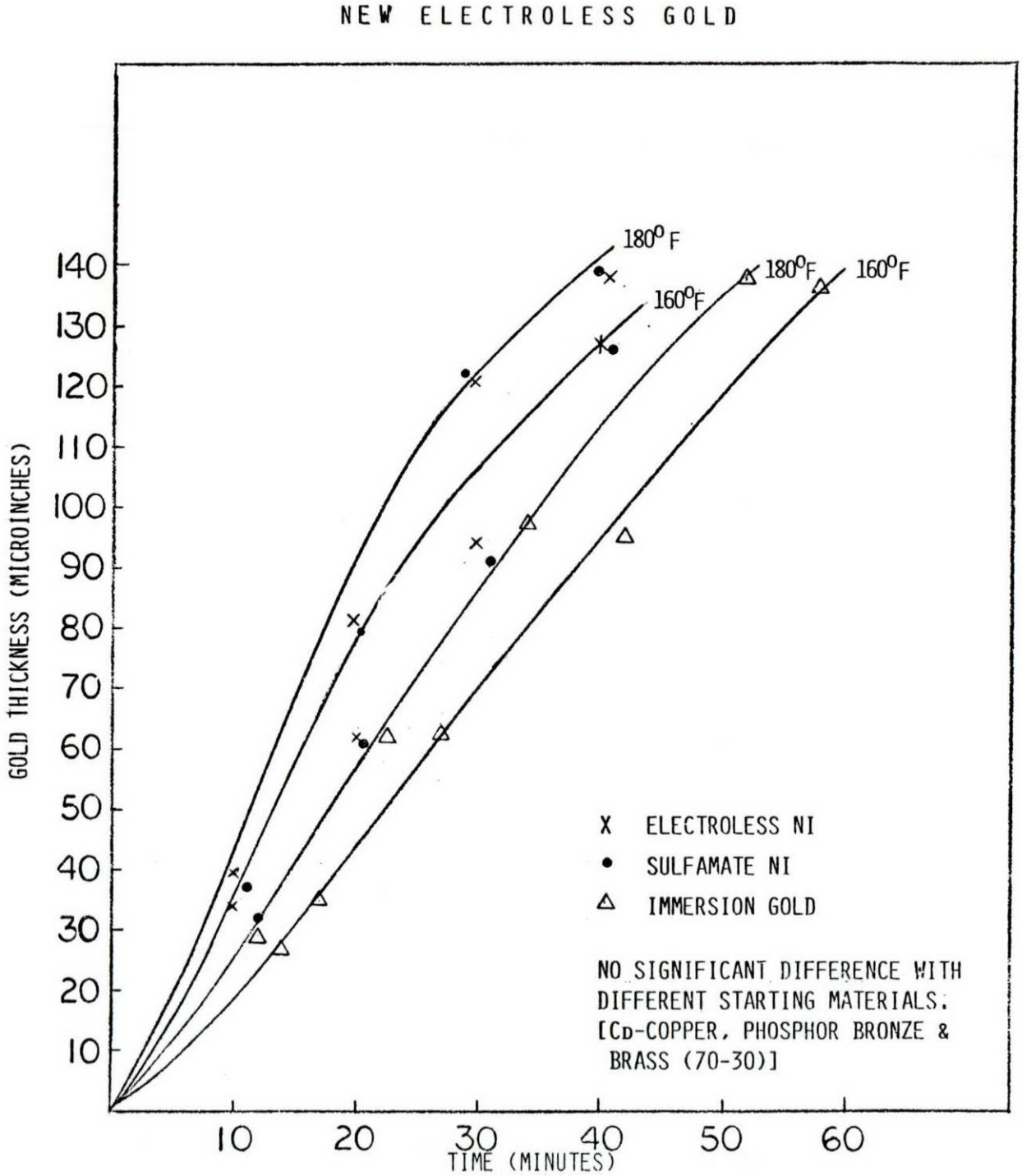

FIGURE 1. SHOWING RATES OF DEPOSITION ON DIFFERENT UNDERPLATINGS

H-5

Electroless Plating
Session H

Electroless Nickel for Stress Corrosion Protection in Power and Petrochemical Plants

Gabrielle Salvago and D. Sinigaglia
Dipartimento di Chimica Fisica
Politecnico di Milano
Milano, Italy

ELECTROLESS NICKEL FOR STRESS CORROSION PROTECTION IN POWER AND PETROCHEMICAL PLANTS

G. Salvago and D. Sinigaglia

Dipartimento di Chimica Fisica Applicata - Politecnico di Milano
Centro di Studio sui Processi Elettrodici – C.N.R. – Milano
P.za L. da Vinci 32 - 20122 Milano – Italy

INTRODUCTION

Usually electroless nickel is considered to be a wear and corrosion resistant coating (1). In most cases, studies in improving the corrosion behavior of materials coated with electroless nickel are aimed at improving the corrosion resistance of the coating considered in and of itself, or at reducing the porosity and defects of the coating upon a given base material. Though correct and valid in and of itself, this philosophy tends, nevertheless, to consider electroless nickel coating as being similar to chromium or ceramic coatings, with fewer air and water pollution problems and without the difficulties in current distribution or the need to grind the coated surfaces.

In effect, electroless nickel has been used as a substitute for hard chromium plating in numerous applications and represents an "ideal" coating whenever the corrosion problem has to do not so much with protecting the plant construction material as to avoiding contamination of the process fluids with corrosion products from the plant itself. This concept, however, does not take full advantage of the real possibilities of electroless nickel in corrosion prevention in plants; in fact, electroless nickel presents the following unique characteristics, with respect to all other types of coatings:

a) Its amorphous or microcrystalline structure, which produces a corrosion and metallurgical behaviour that is significantly different from that of crystalline metals.
b) Good chemical inertia without, however, the excessive brittleness of chromium, ceramic or other coatings.
c) High levels of phosphorus which, in the "corroded" form, i.e. when oxidized to phosphate, is a traditional corrosion inhibitor.
d) The uniformity of the coating and the possibility of applying it "in loco" even on structures of large dimensions and often when coating was not included in the initial design (2).

In addition, one should also consider the general lack of confidence which corrosion specialists have in coatings which can nullify the protective action or even increase the corrosion effect when there are defects, even incidental ones, in the coating itself. It would thus seem extremely useful to investigate the corrosion behaviour of the coated material-defect taken as a whole, in a given aggressive environment.

Localized corrosion, such as stress corrosion (SC), and hydrogen embrittlement (HE), as the result of a corrosive process, have recently become very important, due to the damage that they casue (3). Traditional coatings are ineffective in resolving the problem and can sometimes even be damaging; so they are prohibited by various specification (4). In power plants, there seems

to be difficulty in selecting the materials for heat exchanger structures, mainly because of the "latent" initiation and propagation of localized corrosion. In the case of condensers which operate with river water, some of the most widely used materials are single-phase aluminium brasses; these alloys, however, are susceptible to SC even in water that is not contaminated with ammoniacal substances (5,6). The SC is tied to the alloy chemical composition, particularly to the phosphorus and arsenic content (5); however, an excessive decrease in these elements would lead to dezincification of aluminium brasses. As a result, it is often necessary to resort to more costly materials, such as cupro-nickel or stainless steels which are not, however, immune to localized corrosion (7). Coatings have not been traditionally used in condensers, though this is a sector that would offer extensive applications in the event that one (or more) coatings were discovered which would not decrease thermal conductivity and which, even when incidental defects are present, would allow SC phenomena on brasses to be avoided or at least reduced, thus eliminating the need to use much more expensive materials (8).

In the petrochemical industry, the need to extract oil and natural gas under increasingly more difficult conditions requires the use of high strength steels capable of withstanding the high pressures that are involved (for example, in pipes and joints for deep drilling) (9). The possibility of using high strength steels is limited by the fact that they are susceptible to environmental fracture, the insurgence of which is intensified by the presence of hydrogen sulfide (10). The latter is a typical poison in the recombination of atomic hydrogen, which thus tends to be absorbed by the alloy (causing delayed fractures) or to be absorbed at the crack tips (causing hydrogen assisted SC cracking). Quenched and tempered low-medium alloy steels are one of the types used in this field, though they are susceptible to frequent environmental fractures; use of high alloy steels is of no avail either (9). Traditional metal coatings are usually damaging to the base metal, even when the coating itself is not defective; coatings are often prohibited as, for example, in the NACE specification (4). In the event that particular types of coatings are found (even very expensive ones) which can eliminate or at least reduce the incidence of failures (causing damage in the range of millions of dollar/failure), this would be another field in which such coatings would enjoy widespread use and development.

The aim of this research has been to study Ni-P electroless coatings, of lamellar or collumnar morphologies, applied to aluminium brass or Cr-Ni low alloy high strength steel, from acid or alkaline baths. A Watts type galvanic nickel was selected as a comparison coating. Accelerated SC tests were conducted in appropriate solutions simulating the aggressive environments of a power plant (for brass) and of drilling rigs (for structural steel).

2. EXPERIMENTAL

2.1 Nickel baths

The nickel baths were of the following compositions :

a) Electroless baths. 0.1 M $NiCl_2$, 0.3 M H_3PO_2, 0.2 M citric acid:
   1) - pH 4.3 with NaOH, 1 ppm $PbNO_3$, T = 90°C;
   2) - pH 4.3 with NaOH, 1 ppm MBTA, T = 90°C;
   3) - pH 9.5 with NH_4OH, 1.5 ppm $PbNO_3$, T = 80°C;
   4) - pH 9.5 with NaOH, 1.5 ppm MBTA, T = 80°C.

b) Watts bath. 1.3 M $NiSO_4$, 0.2 M $NiCl_2$, 40 g/l H_3BO_3, pH = 4.0, T = 50°C, 5 A/dm^2.

Reagent grade chemicals and distilled water were used to make all of the solutions.

2.2 Single-phase aluminium brass

The test specimens were 20 mm wide brass rings cut from a 1" heat exchanger tube, in the as-received condition, and of the following chemical composition (Wt %): Cu = 76.00; Pb = 0.002; Al = 2.03 ; Ni < 0.005; Fe = 0.005; Mn < 0.005; Sn < 0.005 ; As = 0.027 ; P = 0.001; Zn = rem.

Therings were diametrically drilled and C - cut longitudinally, according to ASTM G 38-73 specification (11). They then underwent one of the following surface treatments:
- Solvent cleaning (a);
- Wet grinding to grade 1000 SiC paper (b);
- Coating in : bath 1, 3 µm(c) and 20 µm(c'); bath 2, 3 µm(d); bath 3, 3 µm(e); bath 4, 3 µm(f); Watts bath, 4 µm(g) and 15 µm(g').

Before plating, the specimens were cathodically cleaned at 5 A/dm^2 and 60°C in the following solution: 30 g/l Na_2CO_3, 10 g/l EDTA, 10 g/l Na gluconate. The specimens were rinsed and then dipped in a cold 10% H_2SO_4 solution. This was followed by rinsings in distilled water twice. The electroless plating was initiated by suspending the specimens in the electroless bath via an iron wire.

After the surface treatment, the C specimens were bent by tightening a steel bolt centered on the ring diameter so that the brass aluminium yield strength was exceeded in the most strained areas . Phenolic material was used to insulate the specimen from the bolt and, when the tightening was conducted, the bolt was covered with epoxy resin and taped with polytetrafluorethylene. The specimens were bent 1% (with respect to the diameter) in a first series of tests, and 10% in a second series.

For the accelerated SC tests, the following solution was used : 0.1 M Na_2SO_4, 0.05 M $CuSO_4$, 0.005 Cl^-, pH = 3.0, as suggested by (4), to simulate the environment inside an occluded cell (crevice) developed on aluminium brass condensers and other heat exchangers using chloride polluted river water as the cooling medium. The bent specimens were simply immersed in the test solution maintained at 25 ± 0.1°C. In the first series of tests, a time of 144 h was taken, with a surface/volume ratio of 1 cm^2/10 cm^3, and the test solution was changed every 48 h; in the second series of tests, times of 144 h and 312 h were taken, with a surface/volume ratio of 1 cm^2/100 cm^3. At the end of each test, the specimens were diametrically cut and microscopically examined.

2.3 High strength steel

The structural steel (type AISI 4137 H) was of the following composition (Wt%) : C = 0.40; Mn = 0.095; Si = 0.37; P = 0.017; S = 0.016; Cr = 0.99; Ni = 0.16; Mo = 0.18.

The smooth cylindrical tensile specimens (3 mm in diameter) were longitudinally cut from a hot forget casing joint which was mill heat treated by oil quenching from 850°C and tempering at 600°C. Under these conditions, the steel has

the following metallurgical characteristics :
Y.S. = 975 MPa; U.T.S. = 1050 MPa; Elongation = 15%; Reduction of area = 57%; KV = 90 (J/cm^2); HRc = 33; Grain size = 5-8 ASTM.

The specimens underwent one of the following surface treatmens :

- Solvent cleaning (a);
- Coating in : bath 1, 13 μm(b); bath 2, 18 μm(c); bath 3, 13 μm(d); bath 4, 18 μm(e); Watts bath, 40 μm(f).

Before coating, the samples were anodically cleaned at 5 A/dm^2 and 95°C for 1 min in the following solution: 20 g/l NaOH, 20 g/l Na_2CO_3, 20 g/l Na gluconate. After rinsing, the specimens were anodically etched for 20 s at 25 A/dm^2 in a cold 70% H_2SO_4 solution and quickly rinsed in distilled water, no heat treatment was conducted after plating.

For the accelerated SC tests, the following solution was used, as proposed by NACE (4), at room temperature: 5% NaCl, 0.5% CH_3COOH, initial pH = 2.8, H_2S(bubbling).
The tests consisted of placing the unstressed specimens in the aggressive solution and after 30 min stressing and keeping them under a constant tensile load. Measurements were taken of the failure time corresponding to the various applied stress. When no failure occurred, the tests were stopped at 1000 h.

3. RESULTS AND DISCUSSION

3.1 Single-phase aluminium brass

In the first series of tests, the brass, in condition (a), did not reveal any considerable formation of corrosion products; however, the surfase generally appeared to be corroded and cracked with mixed morphologies of cracks (trans- and intergranular) more than 200 μm deep (Fig. 1). The brass, in condition (b), showed considerable copper displacement from the solution and cracks whose depth did not differ significantly from those found in the previous case (Fig. 1).

Regardless of the type of bath (1, 2, 3 or 4), the specimens, coated with electroless nickel, presented considerable copper displacement from the solution, but despite this, no SC phenomena were noted (Fig. 2). The coatings appeared corroded, with the same morphologies already identified in sodium chloride in our previous work (Fig. 2) (12).

The specimens plated with galvanic nickel maintain their original shine; the coating does not display overall corrosion attack, but rather, pitting corrosion can be seen (Fig. 3). In the pits, there is a strong intergranular attack with the SC crack formation; the latter are present even under the unpitted coating (Fig. 3).

Potentiodynamic measurements were conducted on the unstrained specimens in a solution analogous to the one used in SC tests, but with sodium ions being substituted for copper ions (Fig. 4). The anodic behaviour was analogous for all four types of electroless nickel coatings; in particular, in free corsorion,electroless coatings were anodic with respect to the brass (contrary to the cathodic behaviour displayed by galvanic nickel coatings).

The second series of SC tests was conducted on specimens coated with electroless nickel and bent so as to crack the coating and thus expose the base

material as well to the aggressive environment. No SC was ever observed even in correspondence with coating lacerations; these lacerations were often filled by the copper displaced from the solution (Fig. 5). After 312 h, the coating of 3 μm was almost completely "destroyed"; nevertheless, no SC was observed so long as traces of the deposit still remained upon the surface (Fig. 5).

Once the coating had completely disappeared after 312 h, SC began in a manner analogous to uncoated specimens. Coatings that were initially of a greater thickness continued their protective action even after 312 h, despite the non-uniform overall corrosion attack (Fig. 6).

On the basis of the above observations, it would thus seem that SC phenomena in single-phase aluminium brasses are due to crack tip preferential dissolution. The protective action of electroless nickel coatings, which are anodic with respect to the base brass, appear to be that they dissolve preferentially, though not in a uniform manner. Their protective ability (at least as far as thin coatings are concerned) does not seem to be tied to any defects nor to the type of coating bath (either acid or alkaline), but to their slow corrosion rate.

The behaviour of galvanic nickel seems to be the opposite of that of electroless nickel. It is, in fact, cathodic with respect to the base brass; it seems to be susceptible to pitting corrosion, with a stimulation of intergranular attack in the pits; SC phenomena do not appear to be inhibited, not even beneath unpitted coatings.

3.2 High strength steel

The results of SC testing on high strength steel are summarized in Fig.7. Uncoated specimens presented very low failure times and a very low threshold stress level - if it existed. The specimen surfaces appeared corroded and when the applied stress was greater than 30% of the yield strength, gas evolution was visible on the surface (Fig. 8). The fracture appears to be macroscopically brittle; there is, in fact, no necking (Fig. 8). Cracks parallel to the applied stress (= secondary cracks) were observed particularly on the collapsed fracture surface (Fig. 8); no other perpendicular cracks were found. The fracture appeared to be microscopically brittle (Fig. 8).

All of the above leads us to presume that, on the one hand, self-stressing had occurred, as a result of the joint metallurgical history (hot forging, heat treatment); and, on the other hand, that the fracture did not occur because of a crack propagated from the surface towards the inside of the metal (as is typical of stress sulfide cracking), but rather, because of a crack originated and propagated within the specimen, as a result of embrittlement due to the hydrogen absorbed and produced in the corrosive process of the specimen surface (typical of delayed fracture).

Galvanic nickel coatings, due to their lack of macroscopic defects, extend failure time and greatly increase the threshold stress level, without however modifying the form of the applied stress-failure time curve. The fracture appears to be macroscopically and microscopically brittle, but less so than the previous case; the number of secondary cracks seems to be greatly increased (Fig. 9).

Nickel coating obviously modifies the kinetics of hydrogen evolution, which is complementary to the dissolution process; it also alters the stationary

surface conditions between atomic and molecular hydrogen as well as the diffusion kinetics of atomic hydrogen. It can thus be hypothesized that galvanic coatings do not modify the phenomenon of delayed steel failure, but reduce the amount of hydrogen absorption, with a subsequent increase in failure time and in threshold stress, and the maintaining of a certain ductility in the base material.

Electroless nickel coatings from bath 4 seems to have the effect of strongly increasing failure times when stress is highest, without however increasing the threshold stress; they also seem to modify the slope of the applied stress-failure time curve (Fig. 7). Observation of the specimens reveals that the coating has numerous spallings, also as a result of minimal deformations corresponding to a stress level which is 7% of the steel yield strength. Along with these spallings, there is preferential corrosion of the base steel, with the formation of V grooves which degenerate into cracks (Fig. 10). The fracture appears to be macroscopically brittle; furthermore, both secondary cracks and cracks perpendicular to the applied stress appear on the specimen surface (Fig. 10). The fracture reveals corroded areas alongside clearly ductile areas (Fig. 10).

In the case of electroless nickel coatings from bath 3, no failure occurred until 1000 h and until the steel had been stressed to 70% of the yield strength (Fig. 7). The fracture, obtained on the sample stressed at 90% of the steel yield strength, reveals a very small corroded area within a macroscopically brittle area without coating disjoining (Fig. 11); alongside the latter area, there was a macroscopically ductile area with numerous secondary cracks and coating disjoining. Both the macroscopically brittle and ductile areas were microscopically ductile (Fig. 11). In the case of electroless nickel coatings from bath 2 the fracture appear to be analogous to the previous one, but without coating disjoining (Fig. 12).

On specimens coated in the electroless nickel bath - 1, failure did not occur until the steel had been stressed to 90% of its yield strength and until 1000 h. After this time the specimens, subjected in air to a tensile test, reveals a macro and microscopically ductile fracture (Fig. 13).

It can thus be hypothesized that, in the case of specimens coated with electroless nickel from baths 2, 3 and 4, the fracture occurs because of SC or rather, because of a crack (corresponding to coating spalling) advancing, mainly by dissolution, and reducing the resistant section until the specimens collapse. The dissolution process thus appears to be preferentially localized at the crack tip, while the complementary cathodic process of hydrogen evolution appears to be localized on the nickel coating. The latter seems to have very little permeability towards the hydrogen itself. During steel plastic deformation, stress distribution, leading to secondary cracks, seems to also depend upon the coating mechanical behavior.

In one series of test, the specimens were placed in an N_2 deaerated testing solution in which hydrogen sulfide bubbling was begun after 15 min; no stress was applied for 30 min. Then the stress was raised to the yield strength within one hour and maintained at the level until failure. Throughout the test, measurements were taken of the specimen potential (with respect to a saturated colomel reference electrode(connected to the testing solution via a long, double-septum bridge). The results are reported in Fig. 14 and refer to NHE, having assumed E_{SCE} = 240 mV vs NHE.

From Fig. 14, it can be seen that :

- all of the coatings are cathodic with respect to the steel; the galvanic nickel takes on a potential close to the reversible one of hydrogen evolution, while the electroless nickel from baths 1, 2 and 3 is more noble than the latter.
- hydrogen sulfide bubbling mades the coatings become more noble;
- for coatings from baths 1, 2 and Watts, spalling (indicated by the potential lowering) occurs, in these relatively high loading rate, only when the yield strength is reached; for coatings from bath 3, spalling occurs a little earlier.

The fact that the electroless coatings from baths 1, 2 and 3 are more noble than the reversible hydrogen evolution potential, and that they are sufficiently ductile to withstand the static deformation, corresponding to 90% of the steel yield strength for bath 1 and 70% for baths 2 and 3, implies that there is practically no corrosion nor hydrogen evolution, thus explaining the failure lack after 1000 h.

In a final series of tests on specimens coated from baths 1, 2 and 3 and Watts, the following were conducted: Vickers indentations (diagonal of 50 μm), Rockwell indentations (diameter of 200 μm), and diametrical removal of the coating up to 1 mm in width. The coated specimens were then stressed in the aggressive environment to the same level as their threshold stress (Fig. 7); no failure occurred after 500 h.

It can, therefore be asserted that cathodic coating not only reduce the overall corrosion, but also exert a type of "anodic protection" on the steel exposed areas, thus reducing (if not actually impeding) hydrogen evolution on the latter. In addition, particularly for large potential differences and in the presence of small defects, galvanic coupling can contribute to crack tip blunting, by locally stimulating the dissolution process on the base material (Fig. 15), and can thus lead to a stress intensity factor less than the threshold value.

Thus, even in a high-defect situation, cathodic coatings not only do not lead to an increase in SC, but also continue to exert their protective action (though with less effectiveness). In addition, coating defects can easily be identified by potential measurements.

4. CONCLUSIONS

The scepticism and diffidence of corrosion specialists with regard to the application of metallic coatings whenever localized corrosion problems occur, do not always seem justified, despite the fact that it is not always easy to select coatings which are not damaging.

In the case of single-phase aluminium brasses, operating in chloride-contaminated river water (typical of power plants), the SC problems can be reduced by using electroless Ni-P coatings that are anodic with respect to the brass, and thus provide effective cathodic protection. Conversely, galvanic nickel coatings, which are cathodic with respect to the brass, lead to an SC intensification.

In the case of high strength structural steel (type AISI 4137 H), which is used in deep oil and natural gas drilling, the problems of failure (delayed or due to sulfide stress corrosion) can be reduced by ductile nickel coatings

that are cathodic with respect to the steel and which provide a type of effective "anodic protection". Better yet are non-brittle electroless Ni-P coatings that are not only cathodic with respect to the steel, but also more noble than the reversible hydrogen potential and provide the nullification of hydrogen evolution.

It would thus seem that numerous new fields of applications can be found for electroless nickel if, on the one hand, more in-depth knowledge is acquired about corrosion phenomena, and on the other hand, electrochemical-corrosion controls are added to the usual ones now conducted on coatings.

ACKNOWLEDGEMENTS

This work was been performed with a partial financial contribution of the C.N.R. (Progetto Finalizzato C.N.R. - Metallurgia). The authors thank G. Fumagalli for its assistance with the SC tests of aluminium brass.

REFERENCES

1. L.F. Spencer, Metal Finishing, 71, 35 (1974); ibidem, 71, 50 (1974); ibidem, 71, 58 (1974); ibidem, 72, 38(1975).

2. R.H. Fay, A.M. Edmunds, NACE Conference, Houston (1969); Paper No. 86.

3. F.P. Ford, "Stress Corrosion Cracking" in "Corrosion Processes" R.N. Parkins Ed., Applied Science Publishers, London (1982); pp. 271-309.

4. Nace Standard MR -01-75, "Sulfide Stress Corrosion Resistant Metallic Material For Oil Field Equipment".

5. G. Bianchi et al. "Eurocorr. '77" Proceedings of 6th European Congress on Metallic Corrosion, London 19-23 September 1977; pp. 271-278.

6. S. Torchio, Corrosion Science, 21, 59 (1981); ibidem, 21, 425 (1981); ibidem, La Metallurgia Italiana, 73, 274 (1981).

7. VV.AA. - "Advanced Stainless Steels For Sea-Water Application". Proceedings of the Symposium of Piacenza (Italy), 28 February 1980.

8. G. Salvago, Annual Report - Progetto Finalizzato C.N.R. - Metallurgia, 1981, CSM P.O.B. 10747 (Roma).

9. P. Pedeferri, Annual Report - Progetto Finalizzato CNR - Metallurgia 1981, CSM P.O.B. 10747 (Roma).

10. A.W. Thompson, I.M. Bernstein, "The Role of Metallurgical Variables in Hydrogen - Assisted Environmental Fracture" in "Advances in Corrosion Science and Technology", M.G. Fontana, R.W. Staehle Eds., Plenum Press, New York (1980); pp. 53-175.

11. ASTM G 38-73, "Making and Using The C-Ring Stress-Corrosion Cracking Test Specimen".

12. G. Salvago, D. Sinigaglia, et al., International Metal Finishing Conference, Torquay 3-6 May 1978; ibidem, Proceedings 7th International Congress on Metallic Corrosion, Rio de Janeiro 4-11 October 1978, Abraco, Rio de Janeiro 1979, pp. 1716 - 1729; ibidem, Proceedings of World Congress on Metal Finishing 1980, Kyoto 12-17 October 1980. The Metal Finishing Society of Japan, Tokyo, 1980, pp. 162-166; ibidem, Oberfläche - Surface, 22, 232 (1981).

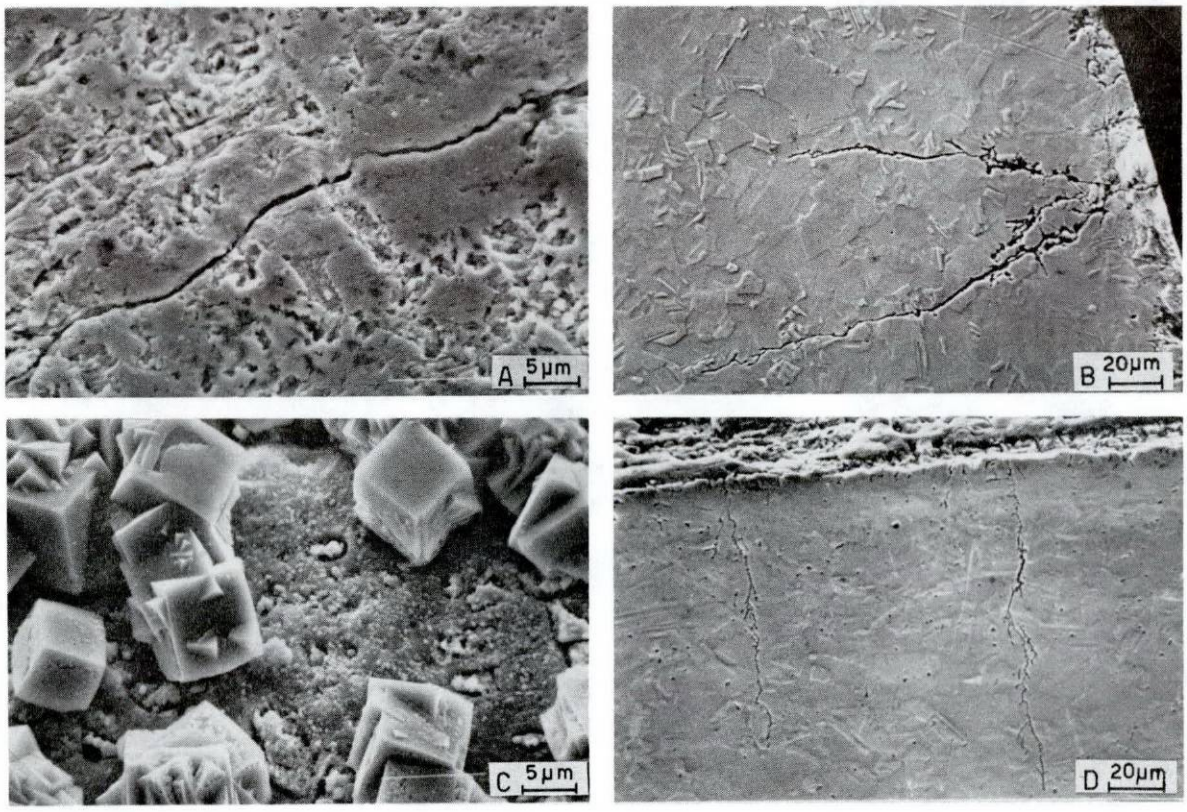

Fig. 1 - Corrosion morphologies of aluminium brass after 144 h SC testing time. As received (A), (B), wet grinding (C), (D) conditions.

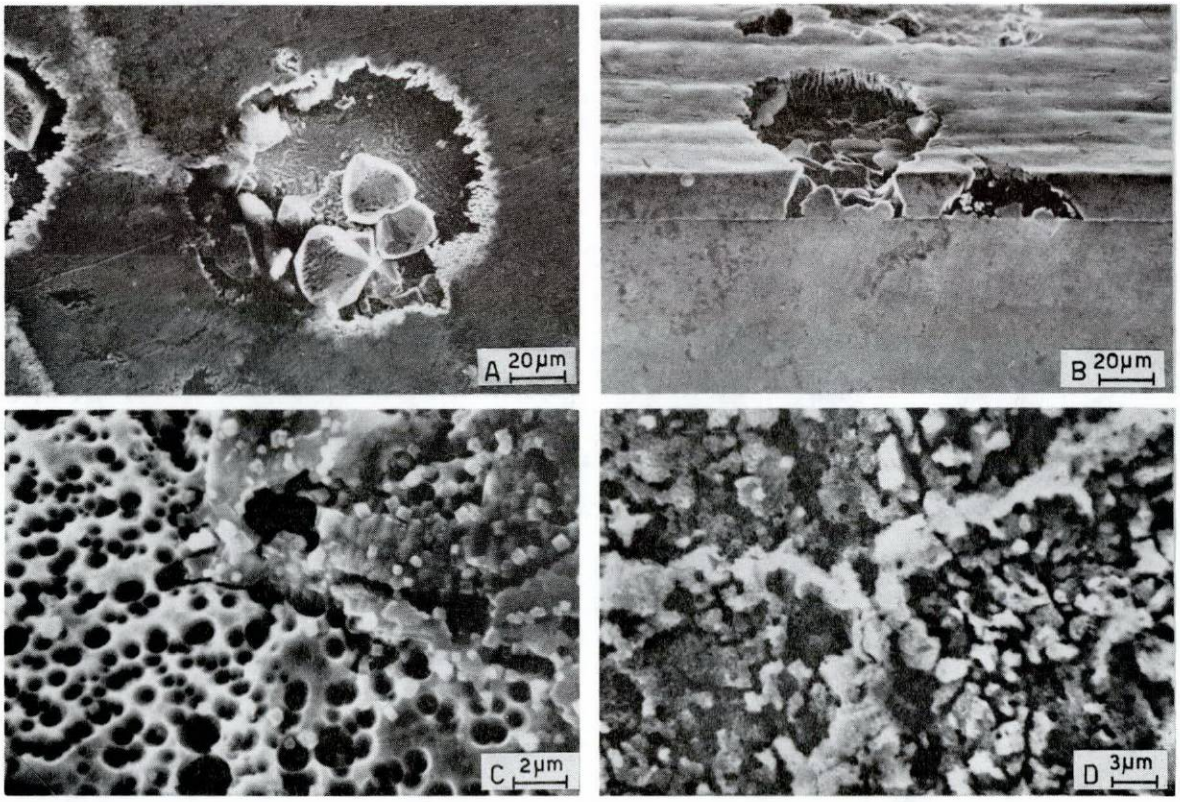

Fig. 2 - Corrosion morphologies of electroless nickel coated aluminium brass after 144 h SC testing time. Bath type 1, 20 µm, (A) (B); Bath type 1, 3 µm, (C); Bath type 2, 3 µm, (D).

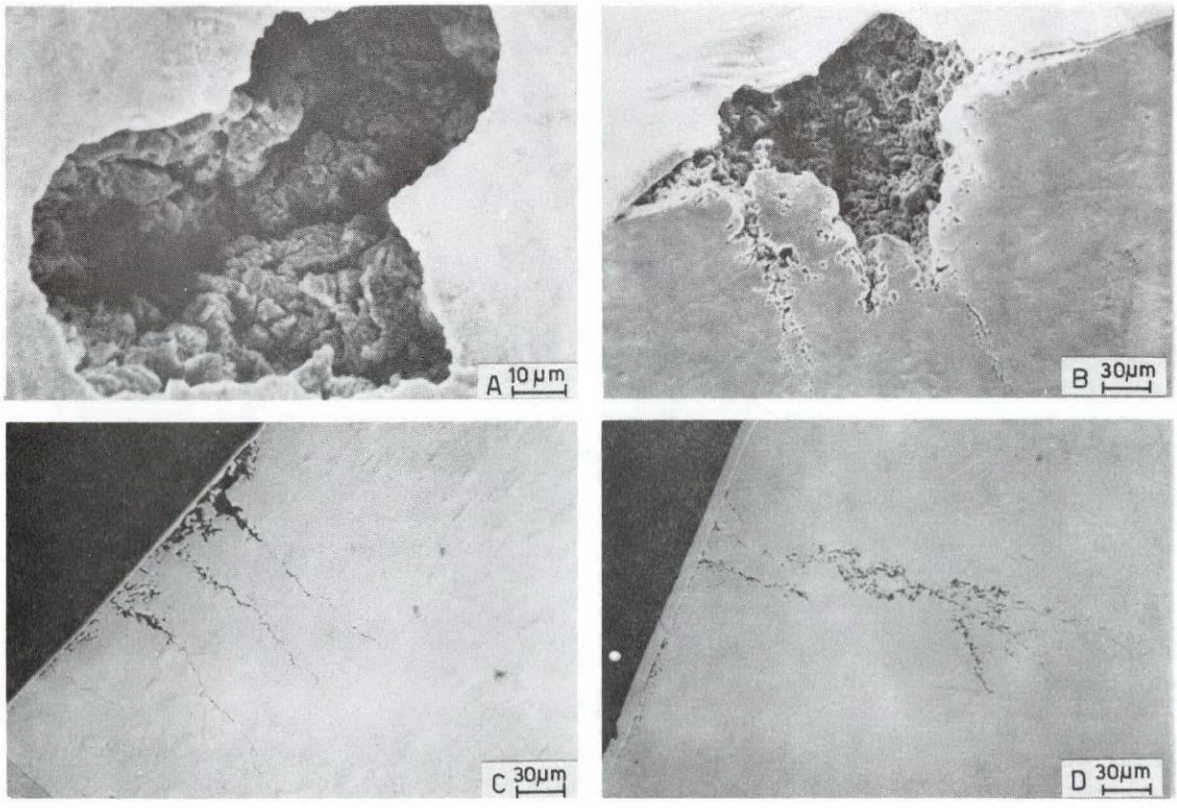

Fig. 3 - Corrosion morphologies of Watts nickel coated aluminium brass after 144 h SC testing time. 4 µm (A), (B), (C); 15 µm, (D).

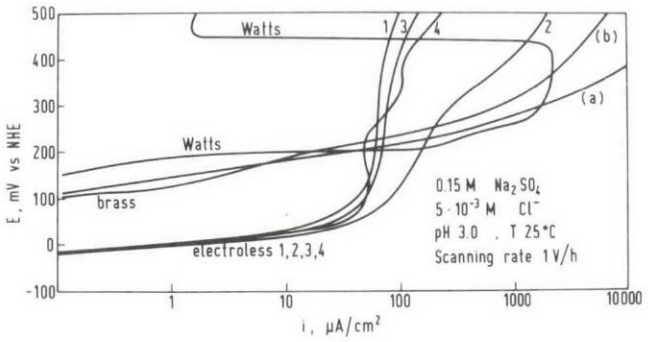

Fig. 4 - Anodic potentiodynamic curves of uncoated and coated aluminium brass in the unstrained condition.

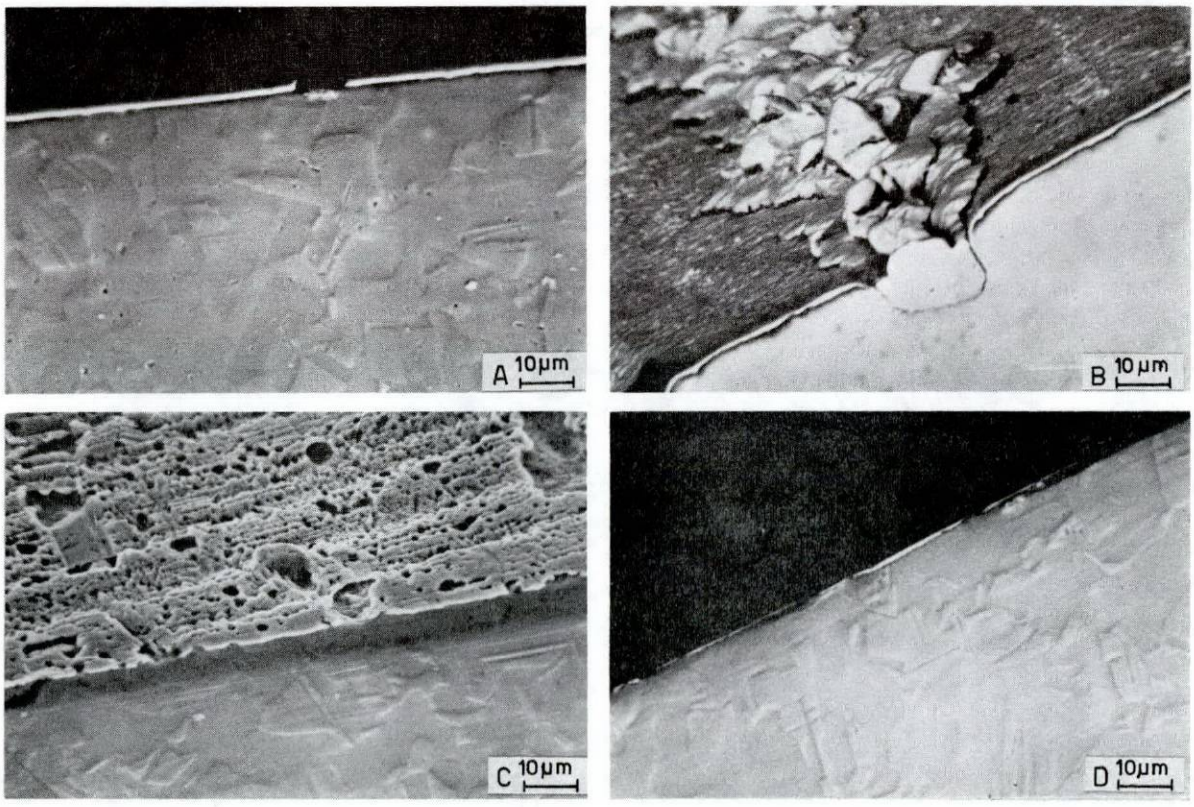

Fig. 5 - Corrosion morphologies of electroless nickel coated aluminium brass (C - specimens bent 10% with respect to the diamter). Bath type 2 (A), and Bath type 4, (B), 144 h SC testing time; Bath type 2, 312 h SC testing time (C) (D).

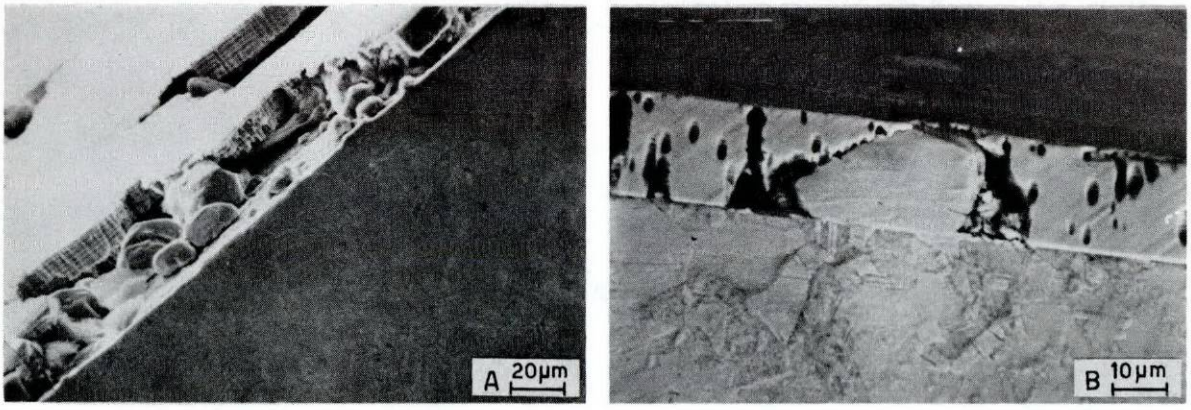

Fig. 6 - Corrosion morphologies of electroless nickel coated aluminium brass. Bath type 1, 20 µm, 312 h SC testing time.

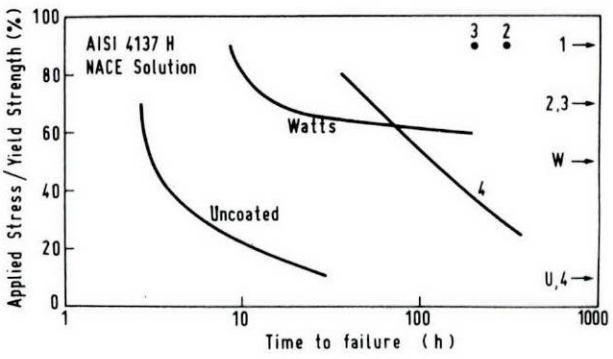

Fig. 7 - Applied stress-failure time curves for uncoated and coated high strength steel.

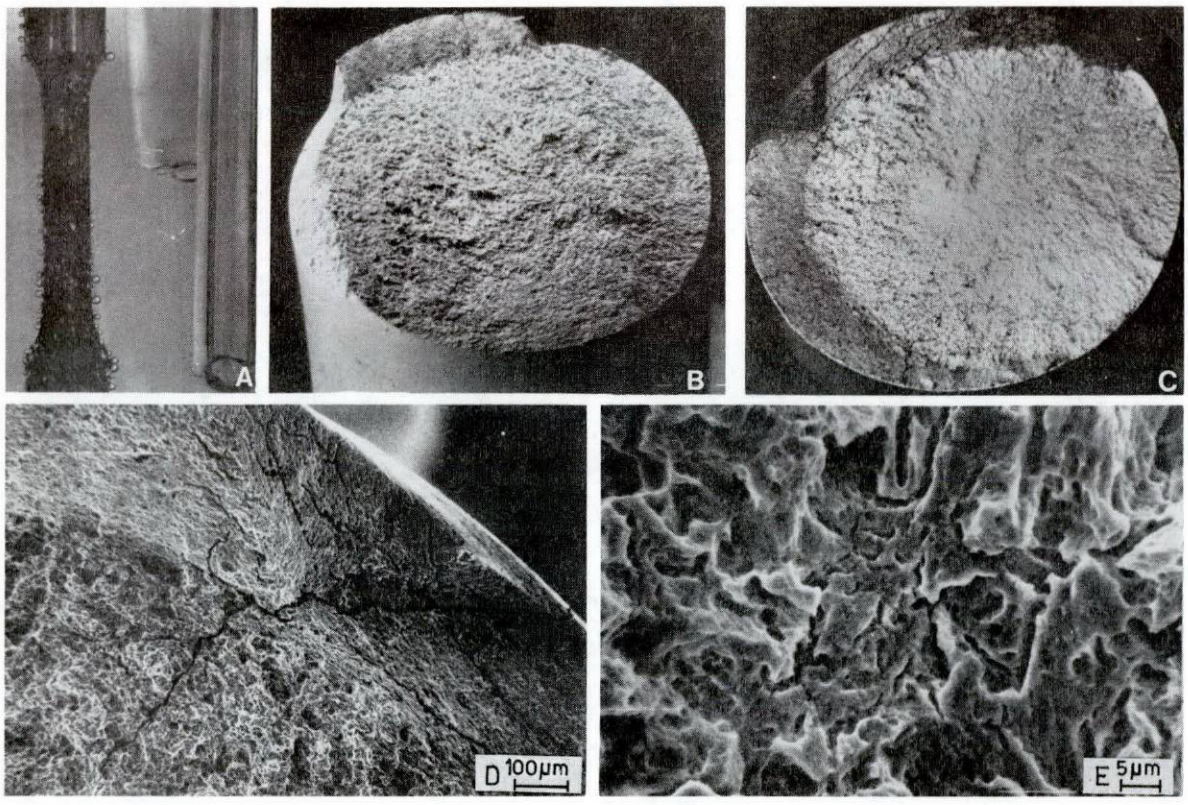

Fig. 8 - Fracture morphologies of high strength steel loaded in NACE solution at: 15% (B), (E); 70% (C), (D), of yield strength.

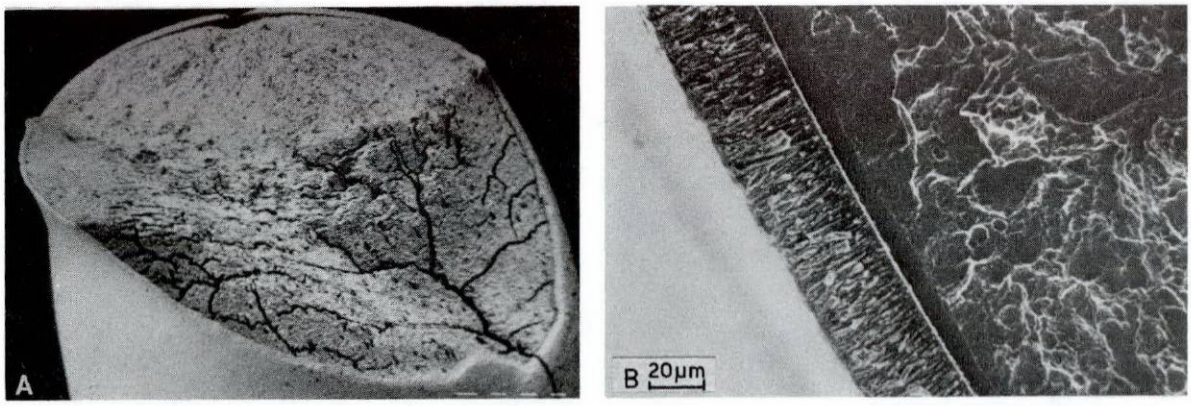

Fig. 9 - Fracture morphologies of Watts nickel coated high strength steel loaded in NACE solution at 90% of yield strength.

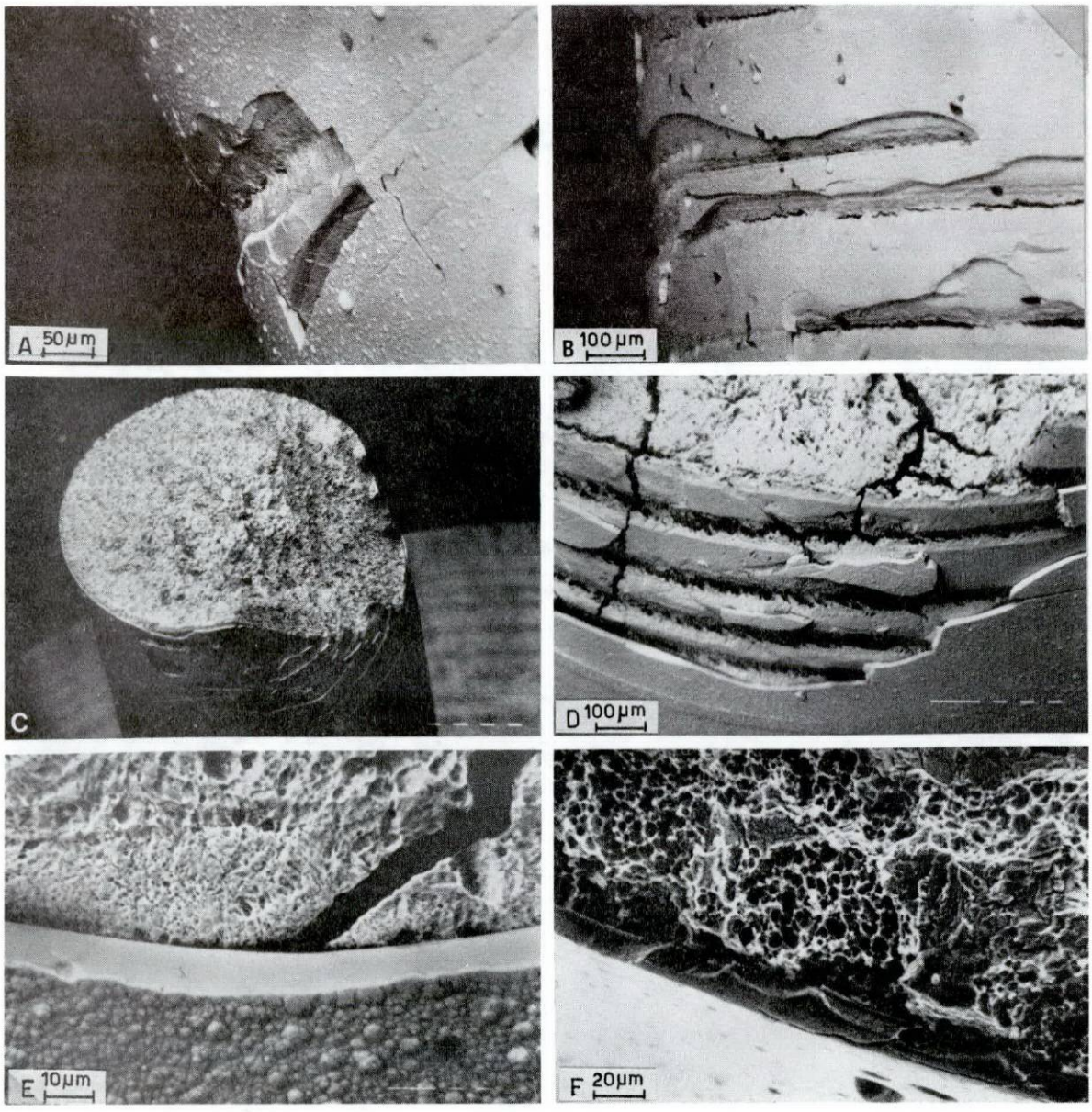

Fig. 10 - Fracture morphologies of high strength steel electroless nickel coated from bath 4 and loaded in NACE solution at : 70%, (A), (B), (D), (E); 50% (C) (F) of yield strength.

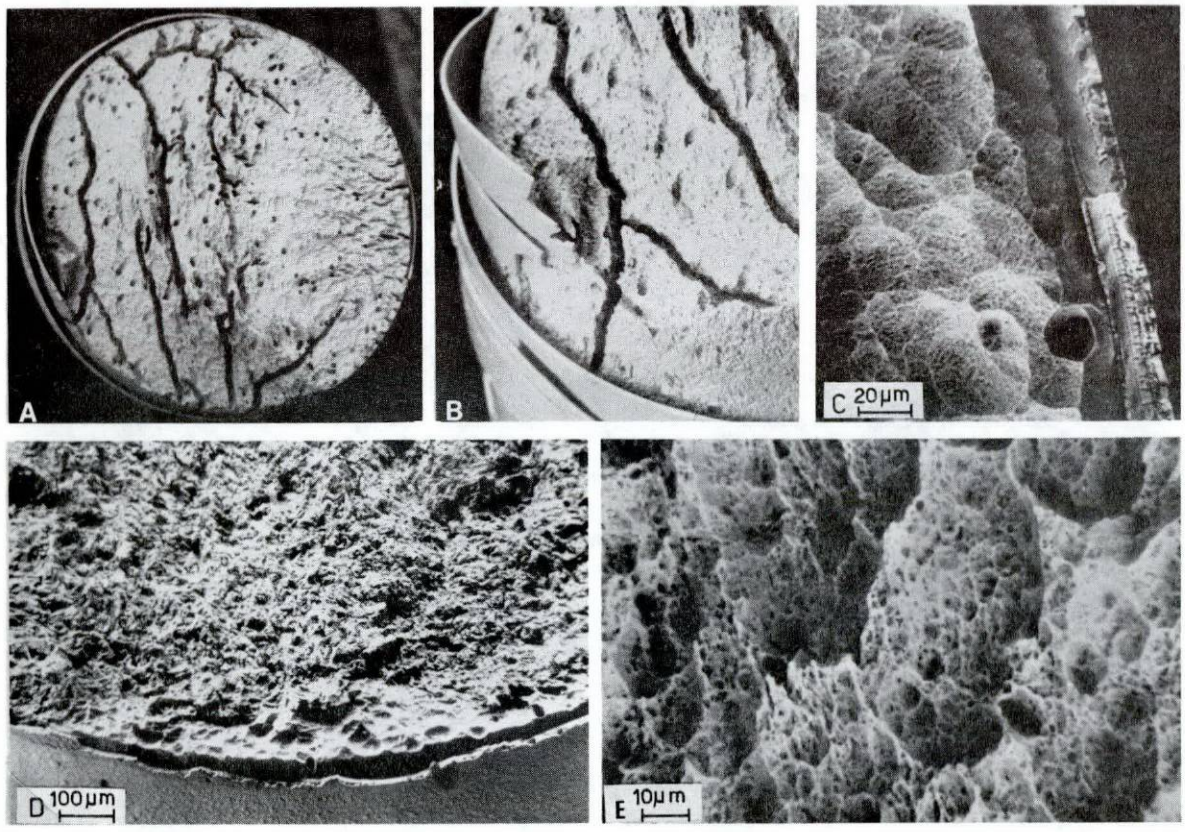

Fig. 11- Fracture morphologies of high strength steel electroless nickel coated from bath 3 and laoded in NACE solutions at 90% of yield strength.

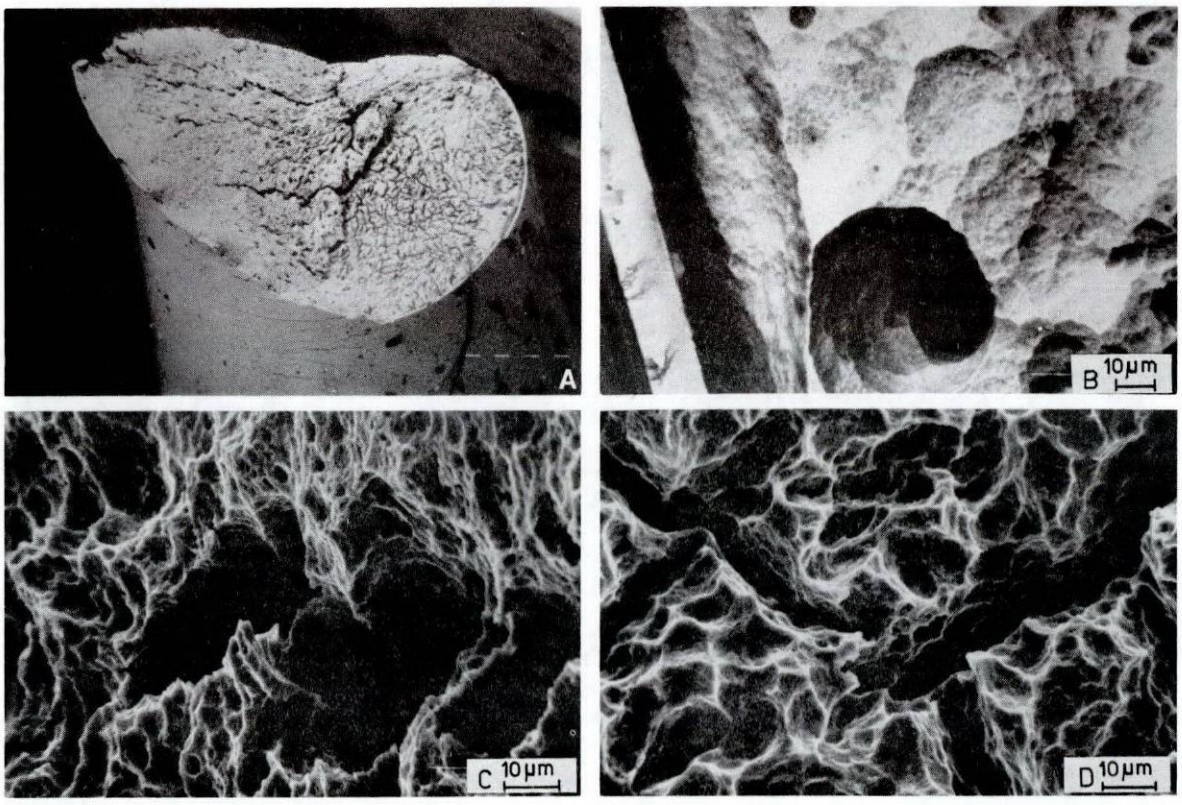

Fig. 12 - Fracture morphologies of high strength steel electroless nickel coated from bath 2 and loaded in NACE solutions at 90% of yield strength.

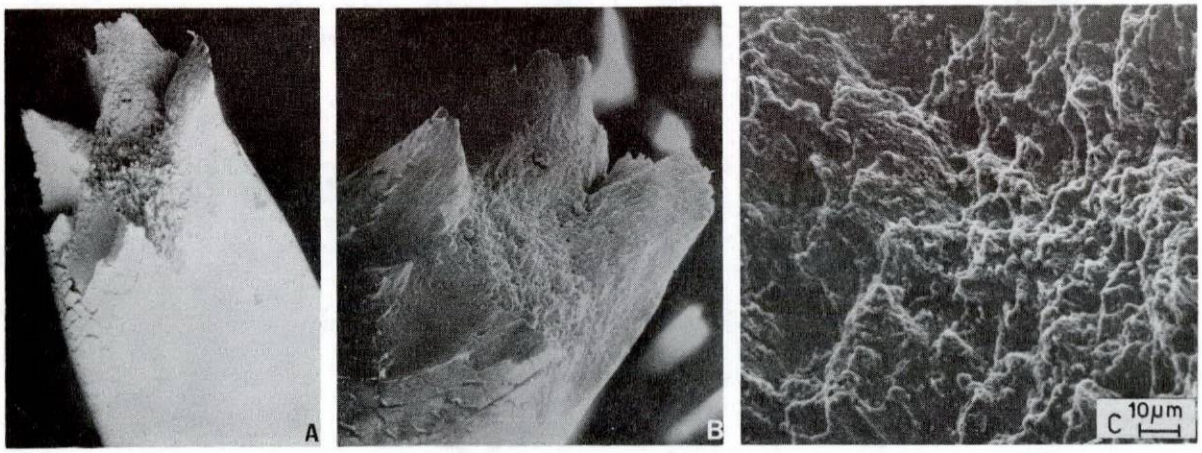

Fig. 13 - Fracture morphologies of high strength steel electroless nickel coated from bath 1, loaded for 1000 h at 90% of yield strength in NACE solution and then tensile tested in air up to ultimate tensile strength.

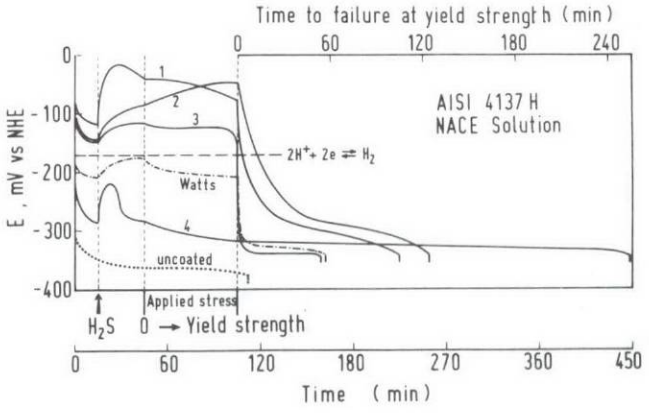

Fig. 14 - Free corrosion potential vs time of uncoated and coated high strength steel.

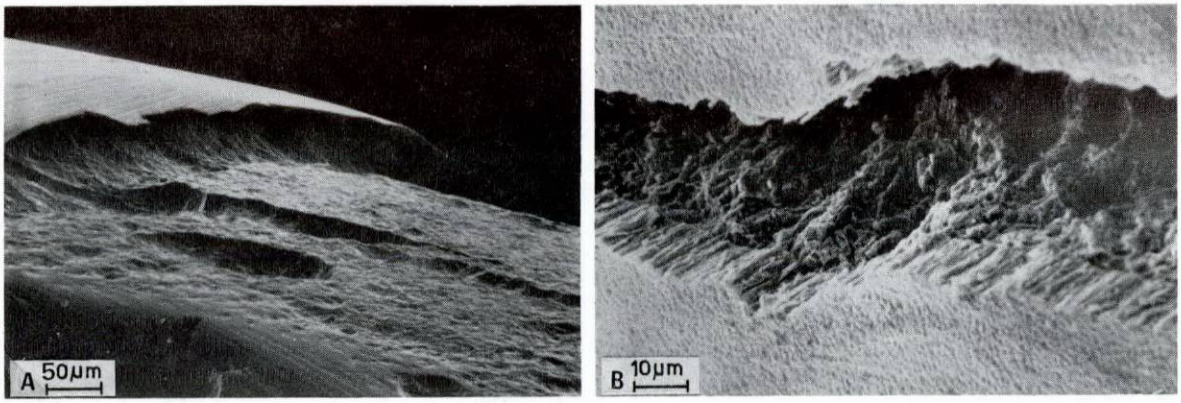

Fig. 15 - Corrosion morphologies of high strength steel Watts nikel coated and loaded at 50% (A) and 100% (B) of yield strength. Mechanical coating removal (A) and crack (B) like defects.

H-6

Electroless Plating
Session H

Diverse Applications for Electroless Tin

Jack Fellman
CuTech, Inc.
Hatfield, PA

Diverse Applications for Electroless Tin

by Jack Fellman
CuTech, Inc., Hatfield, PA

Introduction

Electroless, electrolytic and immersion deposits of tin and its alloys enjoy one common feature in respect to the electronics industry. Functionality. Tin is plated for what it does, not for what it looks like. The scope of this discussion is to present some "old" and "new" applications for electroless tin plating. All of these applications presently involve the use of tin or tin-lead, the difference being the method of applying the metals. These differences will become apparent with each application.

Applications

- Print/Etch

High reliability single-sided boards are being produced for the telecommunications industry by the print/etch process. Requirements for these boards include: solderability, surface electrical properties (dielectric constant) and appearance. Specific utility of these boards is for cable TV boxes and microwave broadcasting equipment.

Process flow for print/etch boards is shown in Figure I.

a. Single-sided copper-clad laminate with 2-ounce foil is the typical starting material.
b. A positive image is screened on the board and the remainder of the ink developed away, leaving exposed copper to be etched.
c. Undesired copper is etched away with either an alkaline ammonia solution or an acid solution, such as persulfate or hydrogen peroxide in sulfuric acid.
d. The etch resist is stripped leaving the circuit pattern remaining on the board.
e. The circuitry is selectively plated with electroless tin to a thickness capable of being reflowed.
f. Boards are reflowed in a hot oil pot at 255°-260°C (490°-500°F) or in an infrared fusing machine. Both reflow processes require a suitable flux.

Conventional technology for producing this type of board is to apply tin-lead by dipping in a molten solder pot and air-leveling or oil-leveling the solder. Another alternative is to use a negative image and electroplate tin-lead as an etch resist and reflow as the final step.

- Flexible Circuits

Light-weight, portable electronic devices such as calculators and watches use flexible circuits in their assemblies. They are produced with the same electrical sensitivity as rigid boards, but on a lighter laminate.

Process flow for flexible circuits is shown in Figure II, which is basically the same as that shown for rigid print/etch boards.

Applications exist where through-holes are punched and plated, as for double-sided rigid boards, followed by pattern plating copper and electroless tin. The final solderable coating is the same for either product, reflowed electroless tin.

- Boards With Solder Mask Over Bare Copper (SMOBC)

a. Etch Resist

Electroplated tin and tin-lead deposits have been used almost exclusively as etch resists for protecting copper circuitry while copper foil is etched away. The deposits are subsequently reflowed as the final solderable coating. In the past two years, board requirements have specified the use of solder mask as a conformal organic coating to protect the circuitry while the product is in use. With the demand for finer lines and spaces, bridging of the solder between two close lines during assembly and wave-soldering has become a problem, since it creates an electrical short. To avoid this, a demand for "no-flow" boards, SMOBC, has become common in the industry. For this type of product, the etch resist is a temporary coating and must be removed after etching.

Typical applications for SMOBC boards are for commercial uses such as computers.

Process flow for SMOBC boards is shown in Figure III. The bare copper board is produced after stripping the tin etch resist. Solder is applied as the final coating on pads and in holes by selective coating with a hot air leveling machine.

b. Solderable Coating Over Copper

Equipment for hot air leveling of solder is expensive to purchase and maintain. A comparable product can be produced by selectively plating with electroless tin, after solder mask has been applied, and reflowing in either hot oil or an infrared machine. The process flow for this modification is shown in Figure IV. In comparision to Figure III, it differs only with the final two steps of electroless tin plating and reflow.

Electroless Tin Process

Electroless tin plating is referred to as a process since it requires surface preparation and activation prior to plating. The precise steps are shown in Figure V.

a. Micro-etch

A brief immersion of the panels in a micro-etch solution is required to roughen the copper surface for good plating. Typical solutions for this function are ammonium or sodium persulfate in sulfuric acid, or hydrogen peroxide in sulfuric acid.

b. Activate

A proprietary copper activator solution is used to assist in the initiation of electroless tin plating. It is formulated around a strong acid and contains organic materials that trigger the electroless plating reaction.

c. Electroless Tin Bath

A proprietary plating solution is used to produce heavy, functional deposits of tin. The bath is mildly acidic, but non-halogenated, and contains tin salts and other components necessary to plate tin. It is operated at 49°C (120°F) with solution agitation and filtration.

Although the bath is electroless in its plating mechanism, it does not suffer from the instability typical of electroless copper and nickel baths. It may be operated indefinitely with proper maintenance and replenishment by a powder product, which allows for a very low cost of operation.

FIGURE I

PROCESS FLOW

Print/Etch Boards With Reflowed Electroless Tin

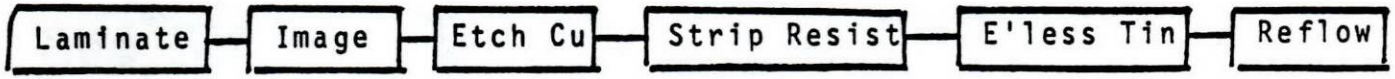

FIGURE II

PROCESS FLOW

Flexible Circuits With Reflowed Electroless Tin

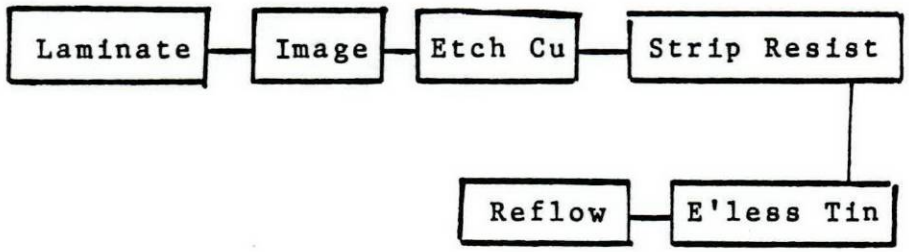

FIGURE III

PROCESS FLOW

SMOBC Boards With Electroless Tin As Etch Resist

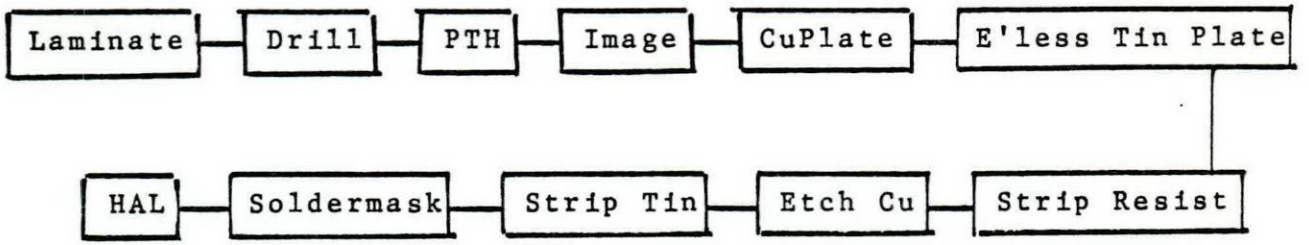

FIGURE IV

PROCESS FLOW

SMOBC Boards With Electroless Tin As Etch Resist
And
Final Solderable Coating

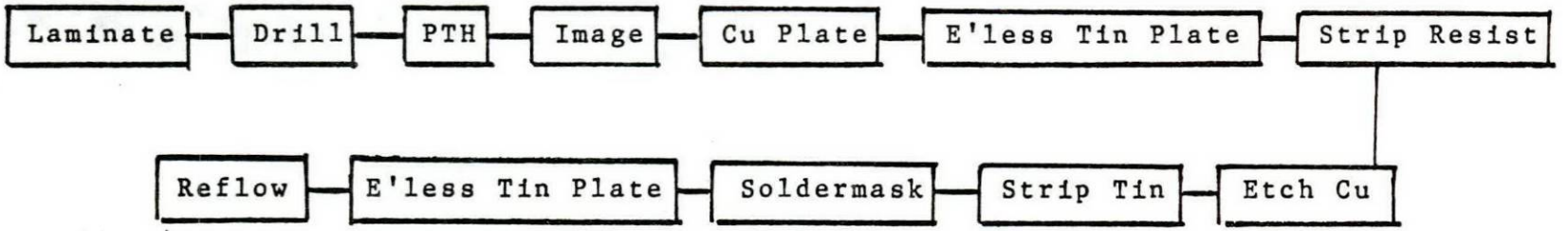

FIGURE V

PROCESS FLOW

ELECTROLESS TIN PROCESS




AMERICAN ELECTROPLATERS' SOCIETY